C. R. Physique 19 (2018) 113–133

Contents lists available at ScienceDirect

Comptes Rendus Physique

www.sciencedirect.com

LEDs: The new revolution in lighting / Les LED : La nouvelle révolution de l'éclairage

Invention, development, and status of the blue light-emitting diode, the enabler of solid-state lighting

L'invention, le développement et l'état de l'art des diodes électroluminescentes à lumière bleue, bases de l'éclairage à l'état solide

Daniel Feezell [a,*], Shuji Nakamura [b]

[a] *Center for High Technology Materials and Department of Electrical and Computer Engineering, University of New Mexico, Albuquerque, NM 87106, USA*
[b] *Materials Department and Department of Electrical and Computer Engineering, University of California, Santa Barbara, CA 93106, USA*

ARTICLE INFO

Article history:
Available online 9 January 2018

Keywords:
Light-emitting diodes
Gallium nitride
Solid-state lighting

Mots-clés :
Diodes électroluminescentes
Nitrure de gallium
Éclairage à l'état solide

ABSTRACT

The realization of the first high-brightness blue-light-emitting diodes (LEDs) in 1993 sparked a more than twenty-year period of intensive research to improve their efficiency. Solutions to critical challenges related to material quality, light extraction, and internal quantum efficiency have now enabled highly efficient blue LEDs that are used to generate white light in solid-state lighting systems that surpass the efficiency of conventional incandescent lighting by 15–20×. Here we discuss the initial invention of blue LEDs, historical developments that led to their current state-of-the-art performance, and potential future directions for blue LEDs and solid-state lighting.

RÉSUMÉ

La mise au point des premières diodes électroluminescentes (LED) bleues en 1993 a marqué le début de plus de vingt années de recherches intensives dans le but d'améliorer leur efficacité. Les solutions qui ont été apportées à des défis critiques associés à la qualité des matériaux, à l'extraction de la lumière et au rendement quantique interne permettent à présent de disposer de LED bleues hautement performantes utilisables pour générer de la lumière blanche dans des systèmes d'éclairage à l'état solide qui surpassent en efficacité les ampoules à incandescence d'un facteur de 15 à 20×. Nous évoquons ici les prémices de l'invention des LED à lumière bleue, l'histoire des développements qui ont mené à la performance de l'état de l'art actuel, ainsi que de potentielles futures directions de recherche en matière de LED à lumière bleue et d'éclairage à l'état solide.

* Corresponding author.
E-mail address: dfeezell@unm.edu (D. Feezell).

https://doi.org/10.1016/j.crhy.2017.12.001
1631-0705/

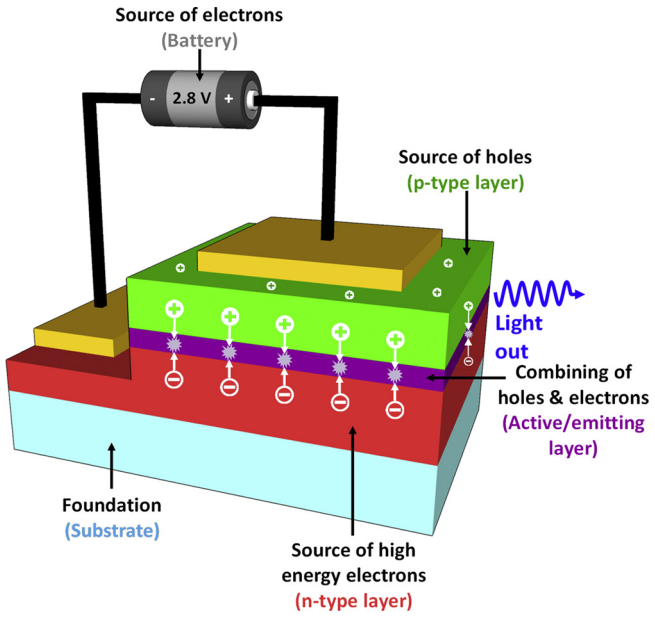

Fig. 1. Schematic of a simple double heterostructure LED, showing the basic operation, substrate, epitaxial layers, and recombination of electrons and holes in the active region to produce photons. Adapted from reference [9]. Copyright 2015 by John Wiley and Sons, Inc. Reprinted by permission of John Wiley and Sons, Inc.

1. Introduction

Lighting accounts for 15–22% of electricity consumption, depending upon the country, and solid-state lighting has the potential to provide enormous energy savings across the globe [1]. In the United States alone, the Department of Energy (DOE) conservatively predicts that solid-state lighting will save 261 terawatt-hours (TW h) annually, representing a 40% reduction in site electricity consumption relative to incumbent technologies such as incandescent and fluorescent [1]. A more aggressive forecast places the annual energy savings from solid-state lighting at 395 TW h by 2030 [1]. At the heart of solid-state lighting are high-brightness, high-efficiency GaN-based light-emitting diodes (LEDs), which represent the state-of-the-art in efficiency, reliability, form factor, and versatility for lighting and displays. The global LED lighting market in 2016 was estimated to be USD 26 billion [2] and commercial solid-state lighting products using GaN-based LEDs are now capable of providing >150 lm/W luminous efficacy and >50,000 hours operating lifetime. However, the development of such high performance LEDs was fraught with complex challenges. Although the first GaN growth was performed using hydride vapor phase epitaxy (HVPE) at RCA Laboratories in 1969 [3], GaN-based materials were not an obvious platform for reliable high-brightness LEDs due to a variety of inherent roadblocks. GaN-based materials initially lacked a native, lattice-matched substrate, leading to large strains and high dislocation densities; p-type doping did not exist; and piezoelectric effects made it challenging to design efficient active regions. With several decades of work, these challenges were largely overcome and Nakamura et al. demonstrated the first high-brightness GaN-based blue LEDs in 1993 [4]. This paper summarizes the historical developments associated with the invention of high-brightness blue LEDs, reviews their current performance, and discusses potential future directions for solid-state lighting. First, we review early breakthroughs that led to high-quality GaN and p-type GaN. Next, we discuss early GaN LEDs and the development of InGaN heterojunction- and quantum-well LEDs. We then summarize later developments on improved light extraction efficiency (LEE) and internal quantum efficiency (IQE), followed by a discussion of white LEDs. Finally, we highlight future directions in visible-light communication (VLC), laser-based lighting, and micro-pixel displays. For further details, we point the reader to several additional accounts of the history of blue LEDs [5–8] and the official Nobel Lecture publications [9–11]. Fig. 1 shows a generic schematic of an LED.

2. Material breakthroughs for high-quality GaN

Several critical materials breakthroughs were needed to set the foundation for the first blue GaN-based LEDs. The development of low temperature buffer layers was particularly important for achieving high quality GaN films since effective buffer layers between the substrate and active layers reduce the dislocation density in materials grown on lattice mismatched substrates. In 1983, Yoshida et al. grew GaN films by reactive molecular beam epitaxy (MBE) using an AlN buffer layer [12]. In 1986, Amano et al. grew GaN films with smooth surface morphology and low residual carrier concentration ($\sim 10^{17}$ cm^{-3}) by MOCVD using an AlN buffer, which was an important milestone [13]. Nakamura et al. later developed a two-flow MOCVD reactor with low carrier gas flow to grow very uniform and high-quality GaN on two-inch substrates [14]. The main breakthrough in this novel design was the use of a subflow, which improved the thermal boundary layer

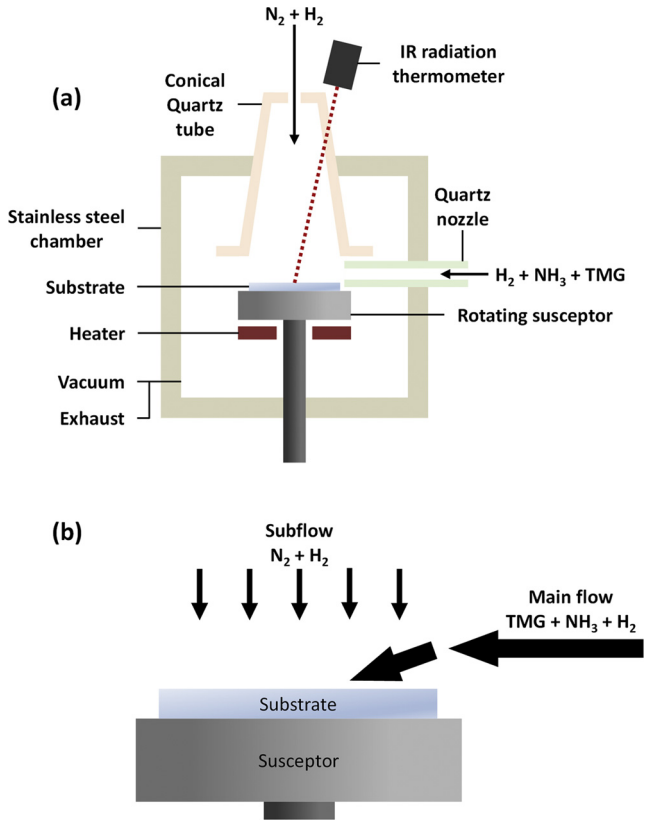

Fig. 2. (a) Schematic illustration of the two-flow MOCVD reactor design. (b) Illustration of the main flow and subflow components. Adapted and reprinted from [14], with the permission of AIP Publishing.

by pushing the carrier gas toward the substrate. Fig. 2a illustrates the chamber design for the two-flow MOCVD, while Fig. 2b shows the main flow and subflow gas directions. The two-flow system sped the development of GaN buffer layers on sapphire substrates using MOCVD [15]. Around the same time, GaN buffer layers were also demonstrated using MBE [16]. Two-flow MOCVD using GaN buffers enhanced the electron mobility to 900 cm^2/Vs in 1992 [17].

A major hurdle toward the development of electrically injected GaN-based LEDs was the lack of conductive p-type GaN. In 1989, Akasaki and Amano achieved a major breakthrough when they applied post-growth low-energy electron beam irradiation (LEEBI) to magnesium doped GaN (GaN:Mg) to realize small areas of electrically active p-type GaN [18]. The physical origin of this breakthrough was not understood until 1992, when Nakamura clarified that hydrogen passivation of Mg dopants was responsible for the low hole concentrations in MOCVD-grown GaN:Mg [19]. First principles calculations were later used to confirm hydrogen passivation in GaN:Mg [20,21]. In MOCVD GaN growth, the nitrogen source is ammonia (NH_3), which dissociates into atomic hydrogen at high temperature. The hydrogen atoms react with Mg to form electrically inactive Mg–H complexes (Mg–H), preventing Mg from functioning as an acceptor. Removal of the passivating hydrogen was necessary to achieve p-type GaN. Indeed, the electron beam in LEEBI caused local heating of the GaN:Mg where hydrogen would diffuse out of the crystal. However, this resulted only in small isolated areas of p-GaN. On the other hand, Nakamura found that thermal annealing of GaN:Mg above 400 °C in an NH_3-free ambient (e.g., N_2 or air) presented a simple and quick method to drive out the hydrogen through diffusion [22], resulting in large areas of p-GaN. The thermal annealing method to activate p-GaN was ultimately commercially adopted due to its simplicity and high throughput.

3. Early GaN-based LEDs

The first GaN-based violet and blue LEDs were fabricated using a metal-insulator semiconductor (MIS) structure due to the lack of p-type GaN. In these n-type forward biased devices, holes are injected from the metal contact through the insulator. These devices were doped with Zn and Mg as color centers and only achieved light output powers of around 70 μW [23–25]. Early LEDs in conventional III–V materials (e.g., GaAs) used simple homojunctions consisting of a single bandgap. The first p–n junction GaN LEDs also consisted of simple homojunctions (see Fig. 3), which do not require alloying with additional elements (e.g., In or Al). The first GaN p-n homojunction LED was demonstrated in 1989 by Amano et al. using an AlN buffer layer and LEEBI treatment to activate the GaN:Mg [18]. The current–voltage characteristics were obtained but the light output power was not reported. This first homojunction LED emitted in the ultraviolet around 365 nm, near

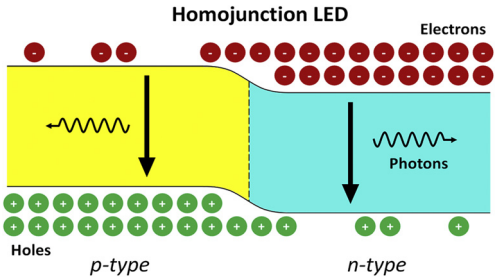

Fig. 3. Energy band diagram of a simple homojunction LED.

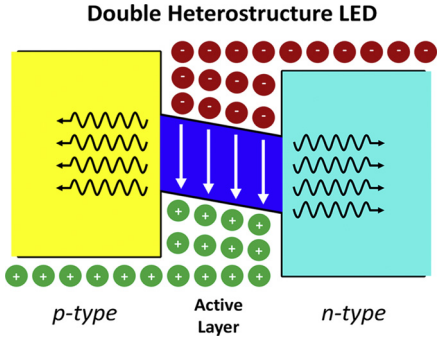

Fig. 4. Energy band diagram of a double-heterostructure LED.

the bandedge emission of GaN. Nakamura et al. also demonstrated a GaN homojunction LED using a low-temperature GaN buffer layer in 1991 [26]. LEEBI was used to activate the p-type GaN in the demonstrations by both Amano et al. [18] and Nakamura et al. [26]. Although the reports of GaN homojunction LEDs marked significant progress in the field, the output powers from these devices were too low (<100 μW) to be useful for real-world applications. In addition, since the LEDs employed only GaN with a constant bandgap, the emission wavelength was fixed around 365 nm. For GaN-based LEDs to have a significant commercial impact, $In_xGa_{1-x}N$ alloys with tunable bandgaps were needed to access the violet, blue, and green regions and to enable the advanced designs necessary to improve carrier confinement and increase output power.

4. InGaN heterojunction and quantum-well visible LEDs

In 2000, Zhores Alferov and Herbert Kroemer shared half of the Nobel Prize in physics for "developing semiconductor heterostructures used in high-speed- and opto-electronics" [27]. A semiconductor heterostructure consists of a junction of two materials with different energy band gaps. The classic example of a heterostructure is $GaAs/Al_xGa_{1-x}As$. The basic heterostructure enabled two-dimensional electron gases (2DEGs), which were leveraged to realize new types of transistors. By extending the single heterostructure concept and arranging the materials in the order of large band gap – small band gap – large band gap, a *double heterostructure* (DH) can be created. This revolutionary concept led to dramatic improvements in LEDs and enabled room-temperature operation of electrically injected semiconductor lasers. Fig. 4 shows an example of a DH. The key advantages provided by the DH are carrier confinement and optical mode confinement. In homojunction LEDs and lasers, diffusion of carriers leads to a low carrier density and the devices operate within the Shockley–Read–Hall (SRH) nonradiative regime. In addition, the population inversion needed for lasing cannot be easily achieved using homojunctions. In contrast, the DH confines carriers to a region that is smaller than the minority carrier diffusion length, allowing the carrier density to increase significantly. The higher carrier density ensures operation in the bimolecular radiative recombination regime and population inversion in lasers is more easily achieved. Optical mode confinement is also provided by the DH since the index of refraction is inversely proportional to the energy band gap. Mode confinement is essential for realizing low threshold gain in semiconductor lasers [28].

Without the invention of the $GaAs/Al_xGa_{1-x}As$ heterostructure, efficient and commercial GaAs- and InP-based LEDs and diode lasers would not have been possible. For GaN-based LEDs to also reach commercially viable performance levels, an analogous double heterostructure design was critically needed. The addition of indium atoms to GaAs to form $In_xGa_{1-x}As$ was already known to reduce the band gap in longer wavelength emitters. Similarly, the addition of indium atoms to GaN to form $In_xGa_{1-x}N$ also reduces the bandgap, enabling heterostructures [29]. By varying the amount of indium, the band gap and emission wavelength are also tunable. In theory, the accessible wavelength range for $In_xGa_{1-x}N$ alloys spans from 365 nm (GaN) to 1771 nm (InN), providing coverage of the entire visible spectrum. However, beyond ∼480 nm the material quality of MOCVD-grown $In_xGa_{1-x}N$ declines continuously due to a variety of inherent materials challenges [30,31], leading

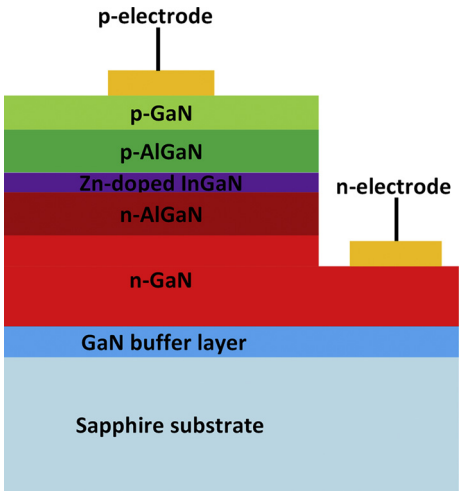

Fig. 5. Device schematic for InGaN/AlGaN double-heterostructure LED.

to the green gap and the use of AlInGaP materials for red LEDs. Nevertheless, $In_xGa_{1-x}N$ alloys are the workhorse materials for violet, blue, and green emitters.

The development of high-quality $In_xGa_{1-x}N$ presented researchers with a number of significant challenges. Although $In_xGa_{1-x}N$ was first realized in 1972 [32,33] and continued to undergo development over the next two decades [34,35], early reports of $In_xGa_{1-x}N$ did not achieve the crystal quality necessary to make active regions in efficient light-emitting devices. For example, emission from deep levels dominated band-to-band emission and x-ray rocking curves showed large (30 min) full width half maximum (FWHM) values. One of the primary challenges with InGaN growth by MOCVD is the high vapor pressure of indium. This high vapor pressure necessitates relatively low growth temperatures (∼800 °C compared to GaN ∼1000 °C) to prevent desorption of indium atoms from the surface. The lower growth temperatures initially resulted in poor crystal quality, which manifested as high levels of impurities and defects that would reduce the luminescence intensity. At these lower growth temperatures, a very uniform and stable temperature profile is required across the wafer. Since indium incorporation depends very strongly on the growth temperature, even slight variations in temperature result in a nonuniform emission wavelength across the wafer (e.g., peak PL wavelength changes by ∼1 nm/°C). In addition, researchers did not yet understand how to achieve smooth $In_xGa_{1-x}N$ morphology and smooth interfaces between GaN and $In_xGa_{1-x}N$, which are both required for the realization of efficient multiple-quantum-well active regions. Another major challenge with $In_xGa_{1-x}N$ growth is the compressive strain experienced by the $In_xGa_{1-x}N$ layers when grown on GaN. Strain management is critical to prevent formation of dislocations.

In 1992, Mukai and Nakamura demonstrated high-quality $In_xGa_{1-x}N$ on a GaN template on a sapphire substrate [36]. The films were grown at temperatures ranging from 780 °C to 830 °C under high TMI flow rates and N_2 carrier gas. The $In_xGa_{1-x}N$ films were 0.3 μm thick. Strong room-temperature, band-to-band photoluminescence was observed for the first time from $In_xGa_{1-x}N$ and the FWHM of the x-ray rocking curve was around 8 min, similar to previously grown GaN films. The researchers credited the custom two-flow MOCVD reactor design and the growth on GaN templates (rather than directly on sapphire) for their realization of high-quality $In_xGa_{1-x}N$ films.

With high-quality $In_xGa_{1-x}N$ layers developed, the last missing piece to a DH GaN-based LED was in place. In 1993, Nakamura demonstrated the first p-GaN/n-InGaN/n-GaN DH LED [37] with an active layer thickness of 20 nm grown on a *c*-plane sapphire substrate. The light output power was 125 μW, the external quantum efficiency (EQE) was 0.22% at 20 mA, and the peak emission wavelength was 440 nm. Fig. 5 shows a device schematic for the first InGaN/GaN DH LED. This first demonstration was followed by further improvements to the blue LED design, including the addition of an AlGaN electron blocking layer (EBL), to prevent electron overflow from the active region, and an increase in the active region thickness to 45 nm. The modified LEDs achieved an output power of 1.5 mW and an EQE of 2.7% at 20 mA [4]. For the first time, blue LED output powers were sufficient for the devices to be commercially viable, prompting the authors of reference 4 to state "high-brightness full-color indicators and flat-panel displays will be developed in the near future."

Although early InGaN/GaN LEDs used DH active regions, a progression toward thin quantum-well active regions was desirable for several reasons. First, the quantum well structure increases the carrier density at a given injected current, which results in the LED operating in the bimolecular recombination regime and improves the radiative efficiency. Second, thick DH active regions are more susceptible to strain relaxation due to the lattice mismatch between the $In_xGa_{1-x}N$ active material and the GaN barriers. Such strain relaxation could lead to the formation of misfit dislocations. Thinner quantum wells are less prone to strain relaxation, which allows for the higher indium contents needed to realize longer emission wavelengths (e.g., green). Third, quantum-well active regions enable tuning of the emission wavelength by simply adjusting the well thickness, which gives engineers additional design flexibility. In 1995, Nakamura et al. demonstrated high-brightness blue, green, and yellow quantum-well LEDs [38]. The green InGaN/GaN LED showed an EQE of 2.1% at 20 mA, which was superior

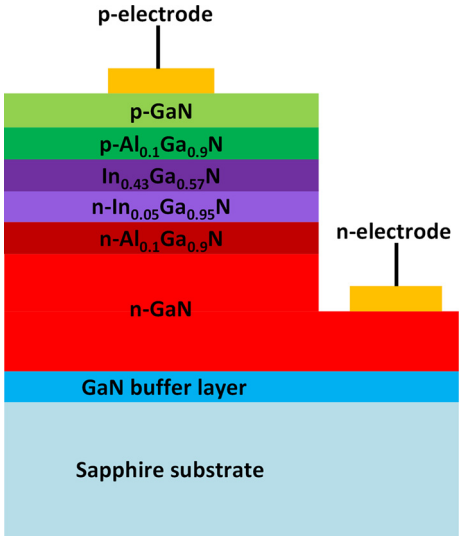

Fig. 6. Single-quantum-well green LED device structure.

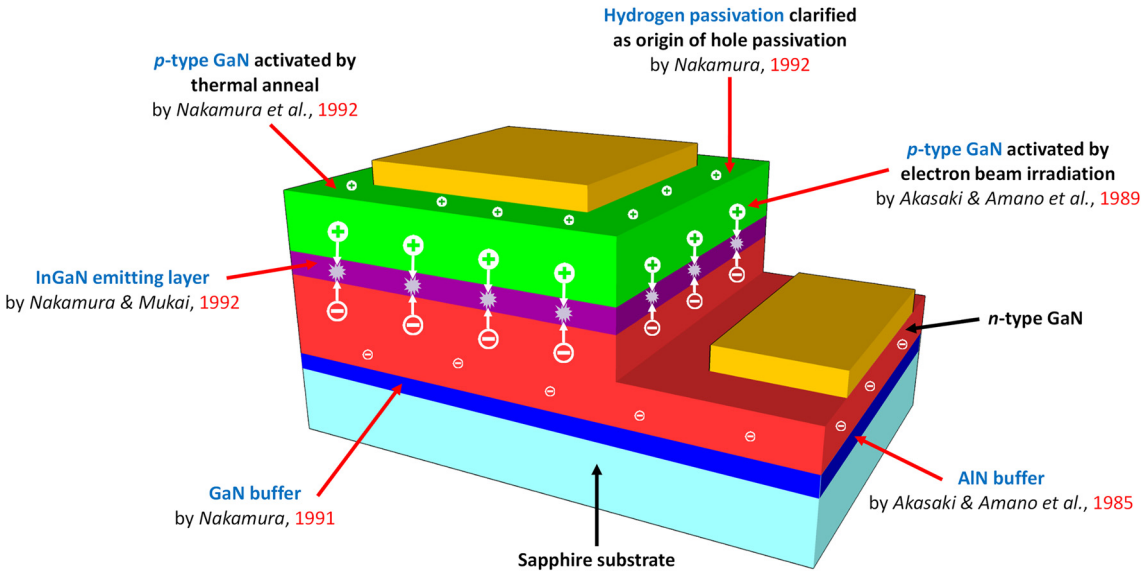

Fig. 7. Summary of important contributions to high-efficiency blue LEDs. Adapted from reference [9]. Copyright 2015 by John Wiley and Sons, Inc. Reprinted by permission of John Wiley and Sons, Inc.

to that of conventional GaP or AlInGaP green and yellow LEDs at the time. In addition, GaN-based materials had superior reliability to II–VI materials, which were the other candidates for fabricating green LEDs. The demonstration of green and yellow InGaN/GaN quantum-well LEDs marked an important turning point in the fabrication of visible LEDs ranging from violet to yellow. It was clear that GaN-based solutions would offer the best combination of efficiency and reliability in the visible region.

Continued improvement in InGaN material quality led to the development of higher power and higher efficiency blue and green single-quantum-well LEDs [39]. A significant modification to the LED design was the use of n-GaN, rather than n-AlGaN and n-InGaN, which improved the quality of the overlying active region by reducing the dislocation density. The 450 nm blue LEDs achieved 5 mW light output power with an EQE of 9.1%, while the 520 nm green LEDs achieved 3 mW light output power with an EQE of 6.3% at 20 mA. Fig. 6 shows the epitaxial structure of these early high-brightness LEDs, which remain the foundation for modern high-brightness LEDs. Fig. 7 gives a summary of the contributions to the development of early GaN-based LEDs.

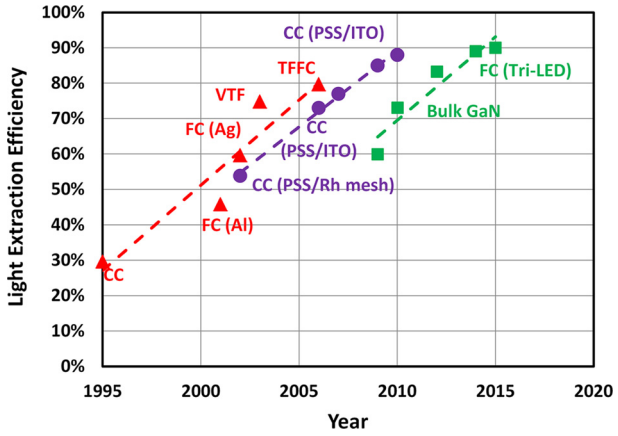

Fig. 8. Evolution of light extraction efficiency over time. Some data points from [31].

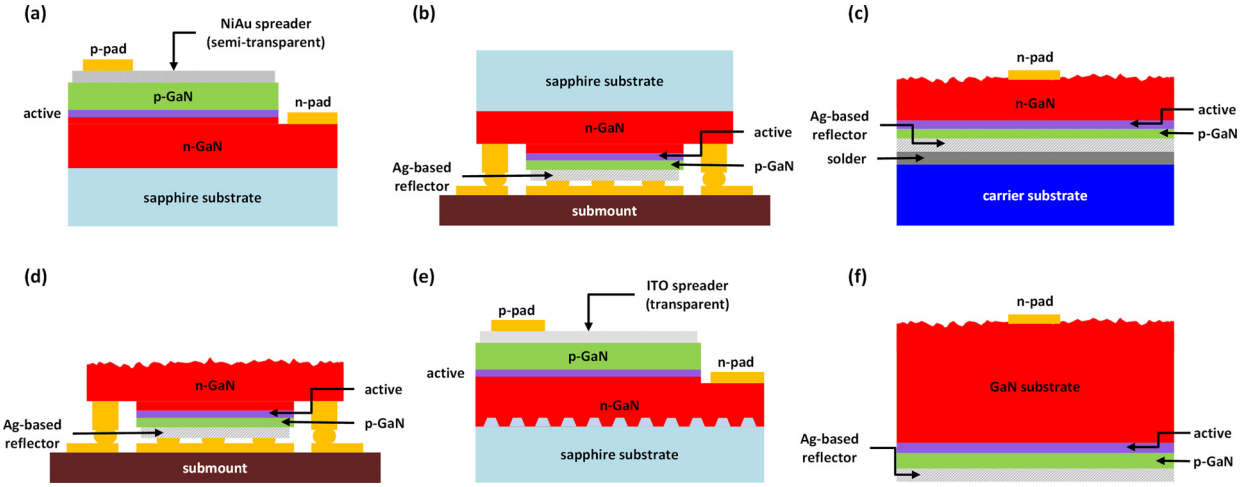

Fig. 9. Various LED chip architectures discussed. (a) Conventional chip (CC) with Ni/Au, (b) Flip-chip (FC), (c) Vertical thin film (VTF), (d) Thin-film flip-chip (TFFC), (e) Patterned sapphire substrate (PSS), and (f) Volumetric chip on quasi-bulk GaN. © 2015 IEEE. Adapted and reprinted, with permission, from [8].

5. Further improvements to InGaN visible LEDs

Beyond the rapid development of high-brightness InGaN/GaN LEDs in 1995, researchers continued to improve the light output power and EQE of both blue and green LEDs through optimized growth techniques, advanced chip designs, and sophisticated packaging schemes designed to increase the LEE and IQE. The realization that blue LEDs could be combined with a commonly available yellow-emitting phosphor to produce white light emission ushered in the era of solid-state lighting [5,40,41]. With the opportunity for a lucrative new market, industry was motivated to devote resources to improve the efficiency of LEDs.

5.1. Light Extraction Efficiency (LEE)

A primary focus between 2000 and 2015 was to engineer higher LEE from the LED chips. The EQE (η_{EQE}) of an LED depends upon the LEE (η_{EXE}) and the IQE (η_{IQE}), where $\eta_{EQE} = \eta_{inj}\eta_{EXE}\eta_{IQE}$. η_{inj} is the injection efficiency. The majority of light emitted within the semiconductor layers is not easily extracted unless special chip designs are employed due to the high index of refraction of GaN ($n_{GaN} \sim 2.5$). For example, a flat surface of GaN emits only around 4% of the incident power due to the total internal reflection (TIR) for light incident beyond the escape cone, and the trapped light is mostly dissipated by the various light absorption mechanisms within the LED [42]. To realize higher EQE, improvements in LEE were required. In general, approaches to achieve high LEE involve surface or interface texturing [43,44], chip shaping [45], and high-index encapsulation [46]. The three main approaches now used for high LEE LEDs are flip-chip with substrate removal, patterned sapphire substrates, and bulk GaN substrates. Detailed discussions of LEE are given in references [42,47,48].

Fig. 8 shows a summary of LEE vs. year for a selection of important chip designs. Fig. 9 shows the schematics for the various III-nitride LED chip designs. Early conventional chip (CC) GaN LEDs primarily extracted light from the p-side

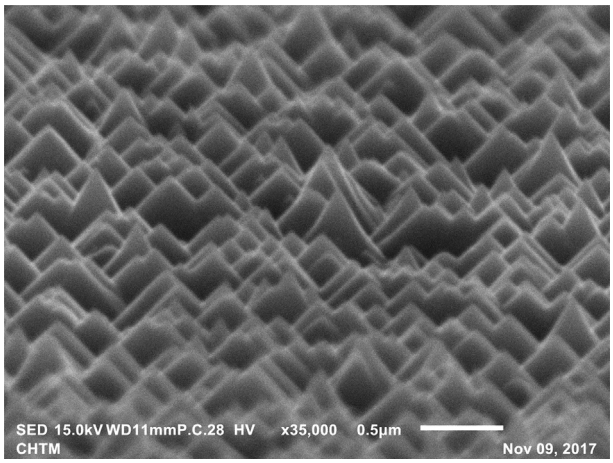

Fig. 10. Scanning electron microscope image of pyramids formed on the nitrogen face after PEC etching.

of the chip. One initial challenge for light extraction was that p-GaN is highly resistive, which prevented current from spreading out underneath the absorbing (opaque) p-side electrode, negatively impacting the LEE. This problem was initially overcome using semi-transparent thin (5 nm/5 nm) Ni/Au current spreading layers to redistribute the current on the p-side of the LED [4]. However, this solution created a trade-off between current spreading and light extraction due to absorption in the Ni/Au layers, and the thin Ni/Au layers could not withstand high current densities without failing, which would ultimately prevent the realization of Watt-class LEDs. Current blocking layers were also developed to improve the LEE by preventing current injection directly beneath the electrodes in p-side-emitting LEDs [49]. Another approach was to fabricate a flip-chip (FC) geometry, where the chip was flipped onto the p-side, bonded to a carrier, and light was extracted through the n-side (backside). The thin Ni/Au p-side electrode was replaced by a thick (∼200 nm) Ag electrode that also functioned as a highly reflecting mirror [50,51]. Ag was preferred over Al because it makes a better ohmic contact to p-GaN and has higher reflectance in the blue spectral region. The thick Ag electrode also enabled the LEDs to operate at higher current densities with better reliability. The flip-chip configuration solved some of the trade-off between light extraction and current spreading and doubled the LEE compared to initial CC designs. However, significant light still remained trapped in the chip due to TIR at the n-GaN/sapphire interface. To overcome TIR at the n-GaN/sapphire interface, the University of California Santa Barbara (UCSB) developed a vertical thin-film (VTF) flip-chip architecture where the sapphire substrate was removed using excimer laser lift-off [43,52]. Substrate removal also revealed the highly reactive nitrogen face of the n-GaN, which was easily roughened using photoelectrochemical (PEC) etching [43]. The resulting surface consisted of nanoscale pyramids with hexagonal bases bound by semipolar $\{10\bar{1}1\}$ facets. Fig. 10 shows a scanning electron microscope (SEM) image of the nanoscale pyramids on the nitrogen face. OSRAM Opto Semiconductors soon developed a product line based on the VTF LED [53]. The addition of surface roughening breaks up guided modes in the thin n-GaN and creates an ergodic surface that randomizes the incident angle of incoming photons and increases the single-pass escape probability [42,54]. The surface-roughened VTF LED exhibited a higher LEE from the top surface by a factor of 2–3× compared to an LED with a flat top surface and showed a Lambertian emission pattern. The total LEE from the VTF LED was estimated at ∼75%. While the VTF LED design achieved a high LEE, the n-contact and a single wire bond remained on the emitting side of the chip above the active region, blocking some of the internal photons from escaping and complicating phosphor deposition. Philips Lumileds proposed a thin-film flip-chip (TFFC) design that placed both contacts on the submount side and improved the LEE to 80% [31,55]. Additional key advantages of the TFFC architecture were excellent heat dissipation and simplified phosphor deposition. The evolution of LEE in the CC, FC, VTF, and TFFC designs is shown in red in Fig. 8.

Around the same time that flip-chip LEDs were initially developed, growth on patterned sapphire substrates (PSS) emerged [56,57]. The PSS technique was originally derived from the epitaxial lateral overgrowth (ELO) technique to reduce dislocation densities, but was found to also greatly improve LEE. By etching microscale or nanoscale features into the sapphire substrate prior to epitaxial growth, the photons are scattered at the sapphire/GaN interface, breaking up guided modes and randomizing the photon directions. Features such as lines, cones, hemispheres, and holes have been demonstrated on PSS [56]. When combined with a semi-transparent indium tin oxide (ITO) p-contact, PSS enabled LEEs close to 90%. Nichia Corporation successfully incorporated PSS and ITO into their LEDs, demonstrating EQEs higher than 84% [58]. The effects of light propagation in the substrate and epitaxial layers, and the impact of pattern density, were thoroughly studied using ray tracing techniques [47]. Light that escapes into the sapphire substrate is easily extracted through the sidewalls because sapphire is nearly lossless and index matched to common epoxies. However, PSS designs are sensitive to absorption in the active region, doped GaN layers, and the ITO contact since photons remain in the epitaxial layers longer due to the low refractive index of sapphire relative to GaN. PSS are commonly used in commercial LEDs because this approach is relatively low cost, does not require the complicated fabrication associated with flip-chip LEDs, and provides very

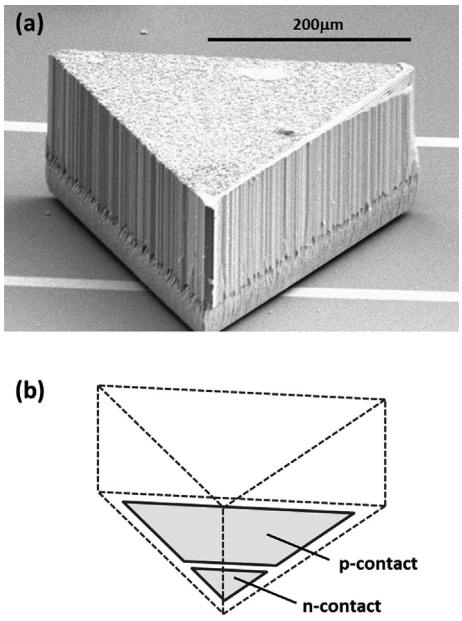

Fig. 11. Flip-chip Tri-LED on quasi-bulk GaN from Soraa, Inc. Roughening is shown on the top surface and sidewalls. Reprinted from [66], with the permission of AIP Publishing.

high LEE. The evolution of LEE in PSS designs is shown in purple in Fig. 8. Note that some of the LEE numbers for PSS were estimated from measured EQE values assuming an IQE ∼0.9.

The availability of free-standing quasi-bulk GaN substrates [59–62] has now enabled volumetric LEDs with vertical-to-horizontal aspect ratios close to unity. Volumetric LEDs extract light from the top surface and sidewalls, which can both be roughened. Soraa, Inc. has developed a bulk-GaN-based volumetric LED with LEE of 90% [63,64]. An SEM image of the Soraa LED is shown in Fig. 11. Two key features of this LED are the flip-chip architecture and the triangular die shape (Tri-LED). The triangular shape breaks the symmetry in the lateral dimensions, frustrating TIR and enabling higher LEE [65]. In addition, both the top surface and the sidewalls are roughened to increase LEE. The Soraa LED emits near 415 nm, where optical losses from the reflecting mirror are relatively high. Thus, the predicted LEE for a similar blue-emitting volumetric LED is as high as 95%, which likely represents the practical limit for GaN-based LEDs [42,66]. The reported volumetric LEDs are grown on low-dislocation-density ($\sim 10^5$ cm^{-2}) quasi-bulk GaN substrates which permit operation at high power (current) densities. Soraa reported 54% EQE at a current density of 1 kA/cm^2. Operation at high current densities is attractive for high-brightness applications. The evolution of LEE in bulk/volumetric GaN designs is shown in green in Fig. 8.

5.2. Internal Quantum Efficiency (IQE)

In many regards, it is extraordinary that InGaN/GaN LEDs are capable of reaching high IQEs (>90%). First, InGaN/GaN LEDs grown on non-native substrates exhibit a high density of threading dislocations ($\sim 10^6$–10^8 cm^{-2}) due to lattice mismatch. With conventional III–V materials (e.g., GaAs or GaP), such a high density of threading dislocations significantly degrades the IQE to essentially zero [67]. However, InGaN is remarkably insensitive to threading dislocations and relatively high IQEs were realized even in the early LEDs [68]. A proposed origin for the insensitivity to threading dislocations is carrier localization due to compositional fluctuations, which would prevent carriers from diffusing to dislocations [69,70]. This explanation is still debated in the LED community, however. Second, despite the presence of strain, high dislocation densities, and high-energy visible photons, InGaN/GaN LEDs do not significantly degrade from new defect formation within the active region during current injection. This is in stark contrast to II–VI emitters, which quickly degrade during electrical injection [71]. The robustness of III-nitrides is attributed to the lack of shear stress on common dislocation glide planes in *c*-plane structures. Finally, large spontaneous and piezoelectric polarization exists in III-nitrides [72–74], leading to internal electric fields that reduce the electron-hole wavefunction overlap and decrease the radiative recombination rate. However, the nonradiative recombination processes were also shown to scale down with the smaller wavefunction overlap by the same factor [75], so the peak IQE is not strongly affected by polarization. On the other hand, the smaller carrier recombination lifetime in *c*-plane structures leads to a higher carrier density for a given current density, causing the maximum IQE to occur at lower current density compared to nonpolar and semipolar structures [76].

Indeed, InGaN/GaN LEDs exhibit a unique behavior known as *efficiency droop*, which refers to the non-thermal roll over of the IQE as the current density is increased. The LED community has invested enormous effort into understanding and mitigating the efficiency droop phenomenon because it prevents efficient operation at high current densities where high lumen densities can be achieved from small-area chips. In general, efficiency droop is commonly observed to differing degrees

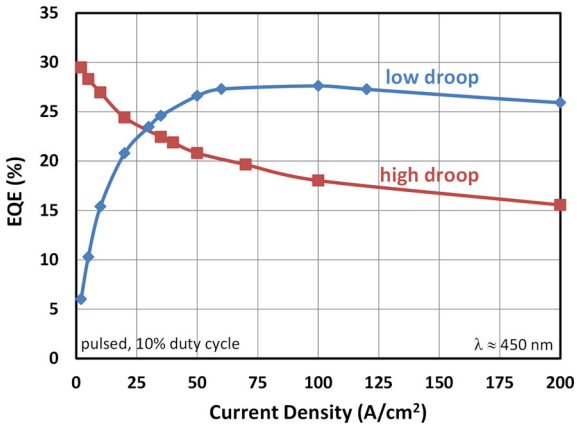

Fig. 12. EQE vs. current density illustrating high and low droop devices.

in both electroluminescence (EL) and photoluminescence (PL), under pulsed and continuous-wave (CW) operation, in both blue and green LEDs, in polar, semipolar, and nonpolar structures, and in multiple quantum well (MQW), single quantum well (SQW), and DH active region designs. In addition, efficiency droop is typically more severe at longer wavelengths such as green and yellow. Fig. 12 illustrates the concept of efficiency droop.

IQE can be expressed in general as the number of photons emitted from the active region per second divided by the number of electrons injected into the active region per second. In terms of the recombination rates and carrier lifetimes, IQE is given by

$$\eta_{\mathrm{IQE}} = \eta_{\mathrm{inj}}\eta_{\mathrm{r}} = \eta_{\mathrm{inj}}\frac{R_{\mathrm{r}}}{R_{\mathrm{r}} + R_{\mathrm{nr}}} = \eta_{\mathrm{inj}}\frac{\tau_{\mathrm{nr}}}{\tau_{\mathrm{r}} + \tau_{\mathrm{nr}}}$$

where η_{inj} is the injection efficiency, η_{r} is the radiative efficiency, R_{r} and R_{nr} are the radiative and nonradiative recombination rates, respectively, and τ_{r} and τ_{nr} are the radiative and nonradiative carrier lifetimes, respectively. Thus, for high IQE, it is desirable to achieve high (low) radiative rate (lifetime) and low (high) nonradiative rate (lifetime). Since the various radiative and nonradiative processes depend upon the carrier density (and by extension, also the current density), an empirical model known as the *ABC model* is often used in IQE analysis, where

$$\eta_{\mathrm{IQE}} = \eta_{\mathrm{inj}}\frac{Bn^2}{An + Bn^2 + Cn^3}$$

Here, n is the carrier density, A is the SRH coefficient, B is the bimolecular radiative coefficient, and C is the Auger coefficient. We note that while quite common, the ABC model has limitations. For example, it assumes the LED is a homogeneous system and does not account for compositional inhomogeneity [77], asymmetry in electron and hole injection in MQW structures, or current crowding [78]. In addition, the ABC coefficients are not categorically constants, since they depend upon the wavefunction overlap, which is a function of carrier density as injected electrons screen the internal electric field, resulting in increased electron–hole wave function overlap. The basic ABC model has been extended to account for the carrier density dependence of the ABC coefficients at high carrier density (i.e. phase space filling) [79,80] and carrier leakage processes [81]. A detailed discussion on the limitations of the ABC model is given in reference [82]. Here we use the basic model to simply illustrate the effects of various types of recombination on LED performance and efficiency droop. At very low carrier densities, the ABC model illustrates that nonradiative SRH recombination (An) is dominant and leads to low IQE. At higher carrier densities the radiative Bn^2 term is dominant and the efficiency increases. At even higher carrier densities, the Cn^3 term dominates, causing the efficiency to decrease. The net effect of the three recombination processes gives rise to IQE curves with the characteristic efficiency droop.

The origin of efficiency droop has been heavily debated, with proposed causes including Auger recombination [80,83,84], carrier leakage [85,86], carrier delocalization and recombination at defect sites [87], and saturation of the radiative rate [88]. After much debate in the LED community, strong recent evidence points to Auger recombination as the primary source of efficiency droop. Shen et al. originally proposed the explanation of Auger recombination for efficiency droop using a photoluminescence technique and ABC model to extract Auger coefficients on the order of $1.4\text{–}2.0 \cdot 10^{30}$ $\mathrm{cm}^6\,\mathrm{s}^{-1}$ [83]. More evidence for Auger recombination was generated in studies using electroluminescence and photoluminescence to obtain the carrier lifetime and ABC coefficients [89–92]. In addition, there now exists theoretical support for the Auger hypothesis [93–96]. A direct measurement of hot electrons associated with Auger recombination was more recently performed [84,97,98]. Iveland et al. studied the electron energies emitted from a commercial LED into vacuum and observed the presence of high energy electrons consistent with Auger recombination at high injection currents. The authors also correlated the missing droop current with the Auger current, providing evidence that the observed high-energy electrons are directly

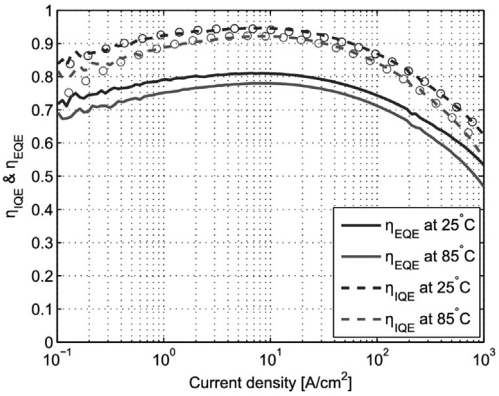

Fig. 13. IQE and EQE vs. current density for Soraa LED on quasi-bulk GaN substrate. Reprinted from [63], with the permission of AIP Publishing.

responsible for efficiency droop. For more in depth discussion of efficiency droop and related mechanisms, we point the reader to several excellent and detailed reviews [82,99–101].

From a practical perspective, there are several approaches to mitigate efficiency droop. Commercial LEDs are commonly based on large-area chips that operate at low current (carrier) density to avoid efficiency droop. The lower carrier density delays the onset of nonradiative recombination associated with the Cn^3 term or any nonradiative process related to high carrier densities. Another approach is to grow thick DH or MQW active regions to lower the carrier density for a given current density. In this case, the peak IQE is shifted toward higher current density where the light output can be maximized. Philips Lumileds was the first group to report DH active regions with peak efficiency at high current density [89]. The DH LED contained a single 13-nm-thick InGaN active region and reached peak EQE at a current density above 200 A/cm^2. This approach has not been widely commercially adopted due to the difficulties in growing thick DH active regions and overall lower efficiency of DH active regions compared to QW active regions due to the lower material quality increasing the A coefficient. In principle, the carrier density can also be lowered by using MQW active regions. Gardner et al. also compared the DH active region to a 6×2.5 nm MQW active region. The MQW active region exhibited a peak efficiency at only $\sim$10 A/cm^2, despite having more total thickness than the DH active region. The result was attributed to lack of hole transport beyond the first p-side QW [102]. Recent precise modeling supports this phenomenon [103].

Using tunnel junctions to cascade multiple active regions together in series is a newer approach to reduce the carrier density without carrier transport issues [104–107]. The addition of tunnel junctions also improves current spreading by replacing the majority of the highly resistive p-GaN with more conductive n-GaN. Improved current spreading prevents regions of high carrier density, resulting in lower efficiency droop. One approach to realize low-resistivity tunnel junctions uses NH_3 MBE to grow $\sim$10–20 nm of highly doped ($[Si] = 2 \cdot 10^{20}$ cm^{-3}) n-GaN on the p++ layer of an MOCVD-grown LED [108]. A low differential resistivity of $1.5 \cdot 10^{-4}$ Ω cm^2 was demonstrated. UCSB utilized this approach on a commercial LED on PSS to demonstrate tunnel-junction-based LEDs with over 70% WPE and low efficiency droop [109]. The tunnel junction approach has also been used to realize GaN-based vertical-cavity surface-emitting lasers (VCSELs) [110] and edge-emitting lasers [111].

Some nonpolar and semipolar orientations have also shown promising performance. For example, low-droop has been achieved in semipolar $(20\bar{2}\bar{1})$ LEDs using 12-nm-thick DH active regions [76]. A study of the *ABC* coefficients in a semipolar $(20\bar{2}\bar{1})$ SQW LED found that the ratio of the radiative coefficient to the Auger coefficient is larger in semipolar $(20\bar{2}\bar{1})$ compared to a similar *c*-plane LED [112]. Both electron and hole transport were also shown to effect the performance of semipolar LEDs, depending on the orientation of the residual built-in electric fields [113]. The major challenge with nonpolar and semipolar orientations is that large-area substrates are not widely available. Also, so far, the maximum IQE of nonpolar or semipolar LEDs has been smaller than that of *c*-plane LEDs.

Finally, we briefly mention two additional techniques that are applied to increase the LED efficiency. EBLs have been shown to prevent carrier overshoot and carrier leakage from the active region [114]. EBLs are typically 10–20 nm thick and composed of AlGaN with 15–30% aluminum. EBLs must be p-doped to reduce the Fermi level and prevent the formation of a hole barrier. Most commercial GaN-based LEDs now contain EBLs. Finally, some LEDs contain a dilute (In $\sim$3%) $In_xGa_{1-x}N$ layer or $In_xGa_{1-x}N$/GaN superlattice layers beneath the active region to improve the efficiency. Armstrong et al. studied the effects of these $In_xGa_{1-x}N$ underlayers on radiative efficiency using carrier lifetime measurements and deep level optical spectroscopy (DLOS) [115]. The underlayers were found to reduce the concentration of deep level defects in the active region, leading to higher radiative efficiency.

5.3. State-of-the-art violet and blue LEDs

Improvements in LEE and IQE have enabled violet and blue LEDs with very high EQE and wall-plug efficiency (WPE). Here we highlight some reports of high-performance LEDs. In 2010, Nichia reported low-output-power (<100 mW) blue LEDs on

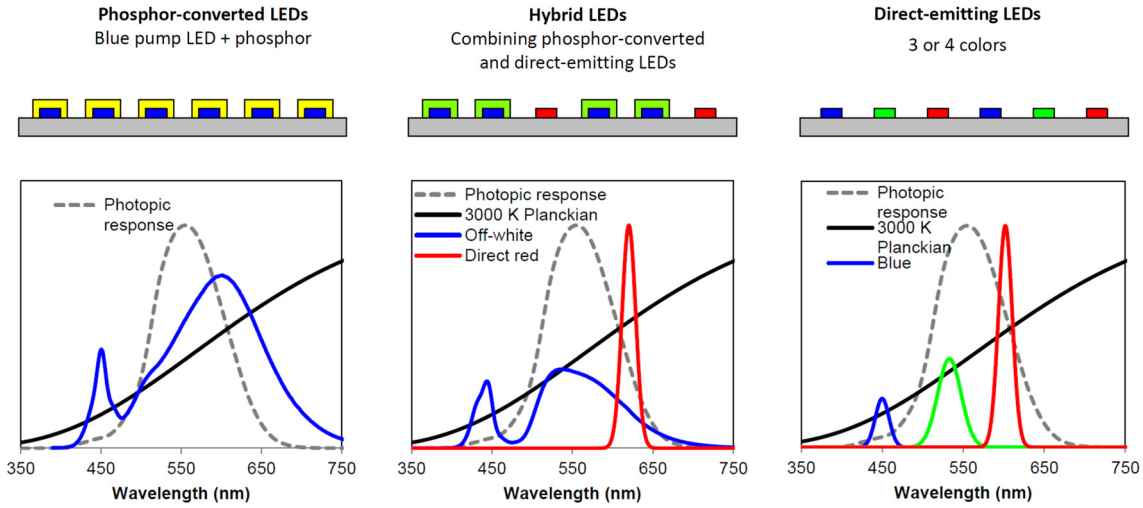

Fig. 14. Three approaches to generating white light using blue LEDs. Figure courtesy of Lumileds from reference [124].

patterned sapphire substrates with an ITO p-electrode with a maximum EQE = 85.9% and a WPE = 81.3% at 20 mA on a 450 × 450-μm^2 chip. A higher power version using a 1 mm^2 chip showed a maximum EQE = 80.8% and an EQE = 76.7% and WPE = 71% at 350 mA (35 A/cm^2) [58]. The high-power LED had maximum light output power around two Watts. In 2015, Soraa, Inc. reported a flip-chip violet (415 nm) LED on a quasi-bulk GaN substrate with peak WPE = 84% at 85 °C [63]. The maximum EQE also reached more than 80%. The LEDs also showed low efficiency droop and the EQE remained above 70% at 100 A/cm^2. Fig. 13 shows the IQE and EQE vs. current density for the Soraa LED for 25 °C and 85 °C.

6. White LEDs

After the initial development of high-efficiency blue LEDs, attention turned to using blue LEDs to engineer white LEDs capable of sparking a revolution in lighting. This new phase in lighting became known as known as “solid-state lighting” and refers to the field of lighting using white LEDs. One implication of solid-state lighting is the replacement of conventional incandescent and fluorescent sources with more efficient LEDs. The energy, economic, and environmental impacts of solid-state lighting are thoroughly discussed by Tsao et al. [116,117]. Here we briefly discuss white LEDs, but a detailed review is given by Cho et al. [118].

The first and most successful approach to create white light using visible LEDs involves combining a blue LED with a phosphor that partially absorbs the blue light and re-emits in a broadband spectrum centered on the yellow region [5,40,41]. The combination of blue and broadband yellow gives the appearance of white light. Associated with the color conversion is an energy loss known as the Stokes-shift loss that is common to all phosphor-based approaches. The blue LED + phosphor approach is illustrated in Fig. 14a. The most commonly used phosphor is cerium-doped yttrium–aluminum garnet (Ce:YAG), which was proposed by Shimizu [119,120]. The blue LED + Ce:YAG phosphor approach has been widely adopted by industry due to its high efficiency, simplicity, stability, and low cost. Nichia Chemical Corporation was the first to commercialize white LEDs in 1996 using this approach [40]. The primary challenge with this approach is that the single phosphor converter emits very little red light, resulting in relatively high color temperatures (5000–6500 K) that gives the light an unpleasant appearance. However, the color temperature can be reduced to 2500–3300 K at the expense of efficiency by adding gadolinium to the phosphor. In some cases, separate red and green phosphors, or full conversion using a combination of red, green, and blue phosphors, may be used. For example, Soraa LEDs emit is the violet region (∼415 nm) and use red, green, and blue phosphors to enable white light products that simultaneously achieve R_a and R_9 values above 90 and low color temperatures [121,122]. This approach trades off lower efficiency droop and better color properties with larger Stokes loss from absorption of higher energy photons within the phosphors.

The second approach uses a hybrid of phosphor-converted and direct-emitting LEDs and is shown in Fig. 14b. A common configuration is the use of partially converted blue LEDs and green phosphor combined with direct-emitting red LEDs. Another configuration involves using direct-emitting blue LEDs combined with phosphor-converted green and red. Although hybrid LEDs with efficient blue and red emitters and efficient narrow-band green phosphors is a practical approach to high efficacy LEDs [82], key challenges with the hybrid approach are obtaining higher efficiency red and green phosphors and narrower band red phosphors [123]. Current red phosphors have broad emission (∼80 nm), resulting in significant light in the far-red region, which reduces lumen output. Reducing the linewidth of red phosphors could increase the lumen output by as much as 20% [124].

For the third approach, direct emission from multi-chip red, green, and blue (RGB) (or RYGB with the addition of yellow) LEDs can be combined in the appropriate power fractions to create white light. This approach is shown in Fig. 14c and was

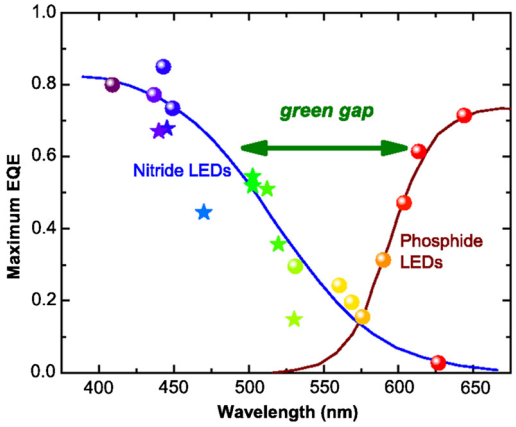

Fig. 15. Maximum EQE vs. wavelength of different commercial InGaN LEDs illustrating the green gap. Reprinted figure with permission from [30]. Copyright 2016 by the American Physical Society.

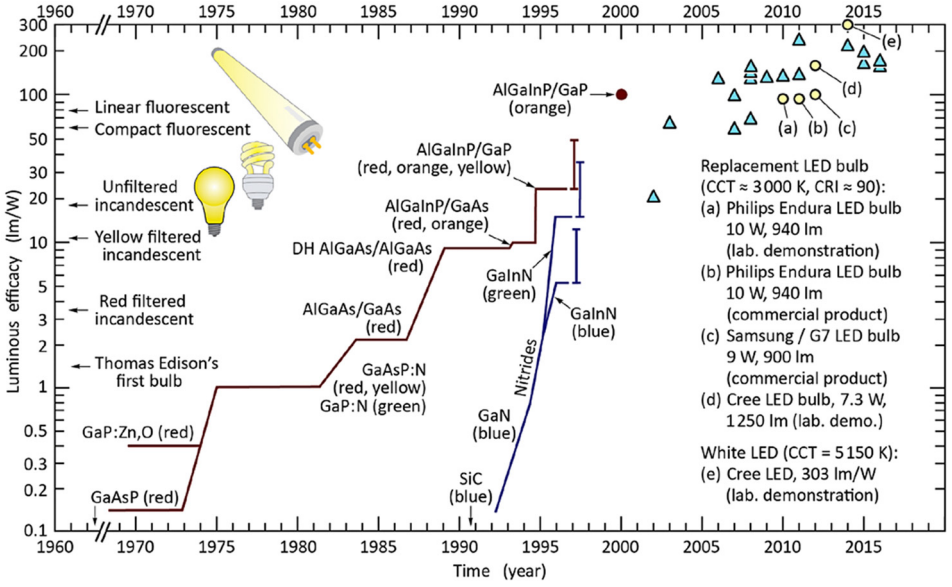

Fig. 16. Evolution in luminous efficacy of conventional lighting sources and visible LED sources. Figure from reference [118]. Copyright 2017 by John Wiley and Sons, Inc. Reprinted by permission of John Wiley and Sons, Inc.

first enabled by the development of efficient blue and green LEDs using InGaN active regions. High-efficiency red LEDs based on the AlInGaP system already existed. The highest possible luminous efficacies can be obtained using this approach, with theoretical maximums in the range of 300–400 lm/W depending on color temperature and color rendering index [125]. A key challenge for this approach is that the efficiency of green LEDs is still quite low compared to those of blue and red. The highest performance InGaN green LEDs show maximum EQEs ~44% at 2 A/cm^2, but still suffer from significant efficiency droop, showing EQEs of only ~30% at 20 A/cm^2 [126]. Alternatively, OSRAM has demonstrated full conversion of a blue LED using a green phosphor to obtain an EQE ~50% at 540 nm [127]. Fig. 15 illustrates the green gap in InGaN/GaN LEDs, where neither nitride-based nor phosphide-based LEDs can currently achieve high efficiency. An additional challenge with color mixing of direct-emitting LEDs is separately controlling the operating conditions (e.g., temperature) of LEDs from two different material systems: InGaN for blue and green and AlInGaP for red.

The evolution of luminous efficacy (lm/W) for visible LEDs and conventional light sources is shown in Fig. 16 [118]. The first white LEDs commercialized by Nichia had a luminous efficacy of 5 lm/W, with some samples reaching 12 lm/W [118]. For comparison, the luminous efficacies of tungsten filament incandescent bulbs, compact fluorescent lamps, and linear fluorescent lamps are ~15 lm/W, ~60 lm/W, and ~80 lm/W, respectively. For LEDs to compete with incumbent technologies, improvements in luminous efficacy were required. In 2004, Nichia reported more than 100 lm/W at very low (<1 mA) currents [128]. In 2006, Nichia reported a luminous efficacy of 174 lm/W at low currents (2 mA) and 138 lm/W at ~20 A/cm^2 [129]. Over the following ten years, further improvements in the efficiency of blue LEDs (described above) led to announcements of laboratory results of 208 lm/W with color temperature of 4600 K at 350 mA by Cree [130], 249 lm/W at

very low current by Nichia [131], 215 lm/W with color temperature of 3000 K by OSRAM [132], and 303 lm/W with a color temperature of 5150 K by Cree [133]. Haitz originally predicted that the lumens per lamp would increase by a factor of 20 per decade [117]. While white LEDs have surpassed this prediction, Haitz's law illustrates the long-term trend of increasing luminous flux over time.

7. Future directions

The solid-state lighting ecosystem has evolved very rapidly over the last few years, with significant improvements in the technical performance of LEDs and the commoditization of LED-based lighting fixtures. The first wave of solid-state lighting based on phosphor-converted white LEDs has already led to commercial products with luminous efficacies beyond 150 lm/W. Furthermore, recent recognition that significant gains in lighting efficiency and functionality can be achieved at a systems level has motivated the industry to pursue so called "smart lighting" systems that will improve energy efficiency, human health, and productivity. These advanced lighting systems will include high-performance light sources, specialized sensors, and dynamic controls to deliver high quality, energy efficient, color tunable lighting with customized spatial delivery and integrated VLC capability [134].

To achieve these capabilities, advanced lighting systems will place greater demands on the performance of light sources. In addition to having energy efficient sources with low droop, sources that provide additional functionalities will be required. Some specific requirements for smart lighting sources include:

(1) low droop for efficient operation;
(2) relatively large ($>$1 GHz) modulation bandwidths for high-speed VLC;
(3) spatial coherence and high beam quality for compatibility with beam shaping/steering elements for customized spatial light delivery and simultaneous illumination/projection;
(4) multi-color (e.g., RGB) configuration for the ultimate efficiency and color tunability and for VLC multiplexing.

Here we highlight emerging device work focused on VLC and discuss the potential of using diode lasers for next-generation lighting systems. In addition, we briefly describe an emerging application for blue and green LEDs in micro-pixel displays.

7.1. Visible-light communication with LEDs

Mobile communications traffic is increasing beyond the limit where radio frequency (RF) technology can support the demand [135,136]. Thus, there is a need for new supplementary wireless technologies to cooperate with existing RF networks [137]. VLC is a promising candidate for next-generation (5G and beyond) network systems, especially for indoor applications [138,139]. InGaN/GaN LEDs are attractive for VLC since they have the potential to simultaneously provide efficient lighting and data communications at minimal extra cost and power consumption [136,140]. However, commercially available highly efficient lighting-class LEDs have low modulation bandwidths ($<$50 MHz) and cannot easily provide the gigabit-per-second data rates needed for VLC. The bandwidth limitation is imposed by three factors: (1) the LEDs are large and have significant RC parasitics; (2) the LED active regions are designed for efficiency, but not speed; (3) the LEDs contain phosphor-based down converters, which have a slow response time. Recently, micro-LEDs (μLEDs) specifically designed for high-speed operation have achieved large modulation bandwidths ranging from 100 s of MHz to 1 GHz, leading to multi-Gb/s data communication rates [141–146]. μLEDs enable high-speed through reduced parasitic capacitance and operation at high current densities where the carrier lifetime is short. To achieve higher light output powers, arrays of μLEDs may be formed. To show the potential for parallel data transmission a CMOS-controlled 8×8 μLED array with individually addressable pixels was demonstrated by McKendry et al. [144,147]. μLED arrays on silicon have also been demonstrated. A key challenge with high-speed LEDs is that they need to operate at high current densities to achieve high speed, which results in significant efficiency droop. Recent studies have focused on understanding the recombination physics and carrier lifetimes in III-nitride LEDs [148,149]. Such studies are relevant to optimizing LEDs for VLC and understanding the trade-offs between speed and efficiency. Nonpolar and semipolar orientations may mitigate the trade-off between speed and efficiency due to their shorter carrier lifetimes at low injection. A detailed review on the use of GaN-based LEDs for VLC is given by Rajbhandari et al. [136].

7.2. Lasers for next-generation lighting

By 1996, further improvements in III-nitride material quality led to the demonstration of the first pulsed [150] and CW [151] violet diode lasers by Nakamura et al. CW blue diode lasers emitting at 450 nm were demonstrated in 2000 on GaN substrates using epitaxial lateral overgrowth (ELO) [152]. Fig. 17 shows a device schematic for the first violet InGaN laser, which contained an InGaN MQW active region and AlGaN cladding layers. A full account of the early history of violet and blue laser development is given by Nakamura, Pearton, and Fasol [5]. More recent InGaN lasers have reached WPE of $\sim$40% and multi-watt output powers [153–157]. III-nitride lasers initially entered the market as sources for high-density optical data storage. Devices with an emission wavelength in the violet region (405 nm) enabled high-density optical disc

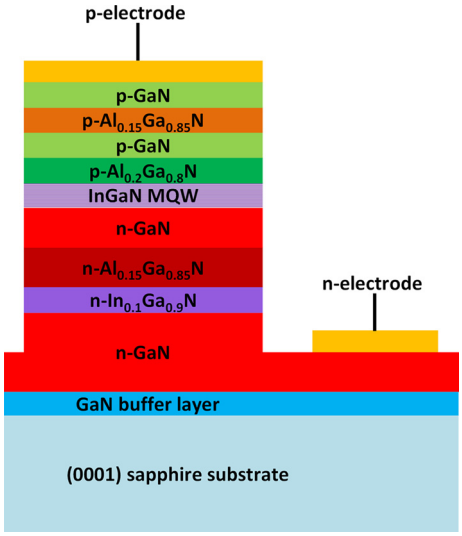

Fig. 17. Device schematic for the first violet InGaN laser.

systems with approximately five times the storage capacity of traditional digital versatile disc (DVD) systems, which utilize 650-nm red lasers. Due to their spectral purity, potential for high WPE, and focus-free operation, lasers are also attractive components for a variety of projection and display systems such as televisions, full-color pico-projectors, and head-up and head-mounted displays.

Recently, InGaN diode lasers have been proposed as next-generation sources in smart lighting systems [158–160] as they provide many beneficial characteristics, including capping of efficiency droop [161], large modulation bandwidths [162,163], spatially coherent output beams, and small form factor. The key ingredients of a laser are a gain medium and a resonant cavity waveguide [28]. The resonant cavity waveguide provides feedback through the gain medium, where stimulated emission causes the photon density to increase rapidly. Above threshold, a laser is dominated by stimulated emission, the linewidth narrows, and a spatially and temporally coherent beam is emitted. Operation based on stimulated emission also ensures a short carrier lifetime, leading to fast modulation speeds (∼5 GHz). The fast modulation speeds of lasers are advantageous for VLC systems to achieve high data rates.

A key advantage of using lasers for lighting is the suppression of efficiency droop above threshold – the laser carrier density clamps due to the high speed of the stimulated emission process. Thus, any rates that depend upon carrier density, such as SRH and Auger recombination and spontaneous emission, no longer increase above threshold. Any new carriers that are added to the laser above threshold recombine in the form of stimulated emission, leading to nearly 100% carrier-to-photon conversion efficiency above threshold. Carrier clamping leads to droop-free operation above threshold, enabling lasers to operate at higher efficiencies at higher input power densities than LEDs. Efficiency droop has a detrimental impact on lighting system design, as it dictates LED operation at low current densities, requiring large device sizes and driving up system costs. Additional advantages of lasers include simultaneous illumination and projection and spatial light delivery when integrated with tunable micro-electro mechanical systems (MEMS) mirrors for beam steering. Already several auto manufacturers are using laser-based headlights, leveraging the small pot size of focused laser light, allowing for precise beam shaping [164]. Fig. 18 illustrates some of the potential advantages of using lasers for next-generation solid-state lighting systems. There are also several challenges with using lasers in lighting systems. First, the current maximum WPE of lasers is only ∼40%, while state-of-the-art WPE for LEDs is ∼80%. Although lasers can be operated at higher current densities where they potentially have an optical efficiency advantage, the large resistive loss at high current densities presents a challenge for higher WPE. On the other hand, lasers are much brighter than LEDs (by a factor of ∼10,000) and the power emitted per chip area is significantly higher (by a factor of ∼20) [157]. This allows lasers to provide higher delivered lm/W in directional applications even with lower WPE. Another issue is that the temporal coherence in lasers leads to random intensity fluctuations known as “speckle.” The presence of speckle is the result of a random interference pattern due to the time coherence of the light source and creates major challenges in using lasers for simultaneous illumination/projection applications. Lasers require light tunnels or optical scramblers to avoid speckle in projection applications. These optical elements increase system cost and lower the light level. The extremely high spatial coherence of lasers also raises issues with eye safety. Finally, the ultra-narrow linewidths (<0.1 nm) of lasers raises issues with their ability to render color properly and with color quality metrics such as R_a and R_f in multi-color RGB-based systems. However, some studies have shown that high color quality is achievable using a four-color laser source [165]. We note that infrared lasers achieved maximum WPE > 70% [166,167] after intensive research efforts. If visible lasers can approach similar WPE, they may offer significant advantages to future lighting systems.

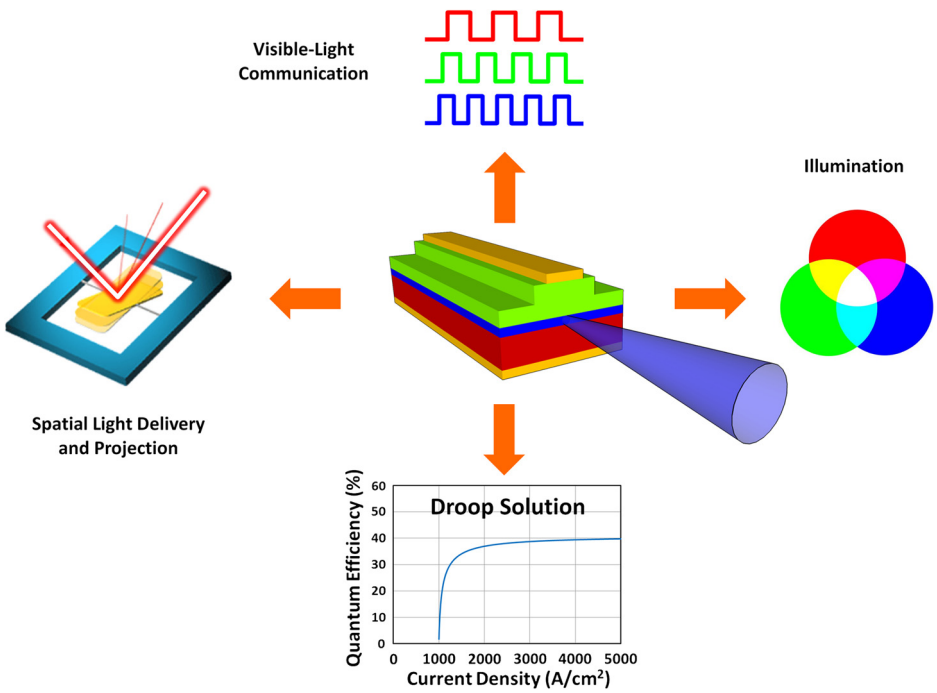

Fig. 18. Illustration of the potential advantages of using lasers for next-generation lighting systems, including illumination, spatial delivery and projection, and visible-light communication. In addition, lasers may provide a viable solution to efficiency droop.

7.3. Micro-pixel LED displays

Another emerging area for GaN-based blue and green LEDs is micro-pixel displays [168–170]. These displays include indoor/outdoor video walls, smart phones, tablets, televisions, and smart watches. Inorganic μLEDs offer potential advantages compared to conventional organic LEDs (OLEDs) and liquid crystal displays (LCDs). Some advantages include higher brightness, higher transparency, longer lifetimes, lower power consumption, and shorter response times. III-nitride based μLEDs exhibit a luminance of 10^5 cd/m^2, while the luminescence of LCDs and OLEDs are 3000 cd/m^2 and 1500 cd/m^2, respectively. Additionally, μLEDs exhibit nanosecond response times, in contrast to the millisecond and microsecond response times of LCDs and OLEDs, respectively [170]. Some μLED displays are based on pick-and-place technology where individual red, green, and blue LEDs are integrated to form a single pixel. Another approach involves using bottom-up nanostructure growth to realize monolithic red, green, and blue LEDs on the same chip by varying the pitch spacing between the nanostructures [171–173]. Apple and Google have recently invested in μLED start-up companies using pick-and-place and monolithic nanostructure technology, respectively [174,175].

8. Conclusion

We have reviewed the historical developments associated with the invention of blue LEDs. The realization of the first high-brightness blue LEDs in 1993 sparked a more than twenty-year period of intensive research to improve their efficiency. After solving critical challenges related to material quality, light extraction, and internal quantum efficiency, current blue LEDs reach WPEs of more than 80%. The application of blue LEDs to white-light generation uniquely enabled the field of solid-state lighting, where white LED sources are now capable of generating luminous efficacies in the range of 200–300 lm/W, a 15–20× increase relative to conventional incandescent technology. Future LED-based lighting systems are expected to include advanced functionalities such as VLC, simultaneous illumination and projection, and integrated controls. Such systems may be tailored to improve energy efficiency, human health, and productivity. Building upon the developments of efficient blue LEDs, efficient blue lasers may be compelling candidates for future lighting systems due to their droop-free operation, high brightness, large modulation bandwidth, and directionality.

Acknowledgement

The authors acknowledge Saadat Mishkat-Ul-Masabih for help with preparing the figures in the manuscript.

References

[1] Energy Savings Forecast of Solid-State Lighting in General Illumination Applications (2014). (Accessed 14 November 2017).

[2] Global LED Lighting Market Size & Trends: Industry Growth and Forecast, 2022 (2017). https://www.zionmarketresearch.com/report/led-lighting-market. (Accessed 14 November 2017).
[3] H.P. Maruska, J.J. Tietjen, The preparation and properties of vapor-deposited single-crystal-line GaN, Appl. Phys. Lett. 15 (1969) 327–329, https://doi.org/10.1063/1.1652845.
[4] S. Nakamura, T. Mukai, M. Senoh, Candela-class high-brightness InGaN/AlGaN double-heterostructure blue-light-emitting diodes, Appl. Phys. Lett. 64 (1994) 1687–1689, https://doi.org/10.1063/1.111832.
[5] S. Nakamura, S. Pearton, G. Fasol, The Blue Laser Diode: The Complete Story, Springer Science & Business Media, 2013.
[6] H. Amano, Progress and prospect of growth of wide-band-gap group III nitrides, in: III-Nitride Based Light Emit. Diodes Appl., Springer, Singapore, 2017, pp. 1–9.
[7] S. Nakamura, S.F. Chichibu, Introduction to Nitride Semiconductor Blue Lasers and Light Emitting Diodes, CRC Press, 2000.
[8] S. Nakamura, M.R. Krames, History of gallium-nitride-based light-emitting diodes for illumination, Proc. IEEE 101 (2013) 2211–2220, https://doi.org/10.1109/JPROC.2013.2274929.
[9] S. Nakamura, Background story of the invention of efficient InGaN blue-light-emitting diodes (Nobel lecture), Angew. Chem. Int. Ed. 54 (2015) 7770–7788, https://doi.org/10.1002/anie.201500591.
[10] I. Akasaki, Blue light: a fascinating journey (Nobel lecture), Angew. Chem. Int. Ed. 54 (2015) 7750–7763, https://doi.org/10.1002/anie.201502664.
[11] H. Amano, Growth of GaN layers on sapphire by low-temperature-deposited buffer layers and realization of p-type GaN by magesium doping and electron beam irradiation (Nobel lecture), Angew. Chem. Int. Ed. 54 (2015) 7764–7769, https://doi.org/10.1002/anie.201501651.
[12] S. Yoshida, S. Misawa, S. Gonda, Improvements on the electrical and luminescent properties of reactive molecular beam epitaxially grown GaN films by using AlN-coated sapphire substrates, Appl. Phys. Lett. 42 (1983) 427–429, https://doi.org/10.1063/1.93952.
[13] H. Amano, N. Sawaki, I. Akasaki, Y. Toyoda, Metalorganic vapor phase epitaxial growth of a high quality GaN film using an AlN buffer layer, Appl. Phys. Lett. 48 (1986) 353–355, https://doi.org/10.1063/1.96549.
[14] S. Nakamura, Y. Harada, M. Seno, Novel metalorganic chemical vapor deposition system for GaN growth, Appl. Phys. Lett. 58 (1991) 2021–2023, https://doi.org/10.1063/1.105239.
[15] S. Nakamura, GaN growth using GaN buffer layer, Jpn. J. Appl. Phys. 30 (1991) L1705, https://doi.org/10.1143/JJAP.30.L1705.
[16] T. Lei, M. Fanciulli, R.J. Molnar, T.D. Moustakas, R.J. Graham, J. Scanlon, Epitaxial growth of zinc blende and wurtzitic gallium nitride thin films on (001) silicon, Appl. Phys. Lett. 59 (1991) 944–946, https://doi.org/10.1063/1.106309.
[17] S. Nakamura, T. Mukai, M. Senoh, In situ monitoring and hall measurements of GaN grown with GaN buffer layers, J. Appl. Phys. 71 (1992) 5543–5549, https://doi.org/10.1063/1.350529.
[18] H. Amano, M. Kito, K. Hiramatsu, I. Akasaki, P-type conduction in Mg-doped GaN treated with low-energy electron beam irradiation (LEEBI), Jpn. J. Appl. Phys. 28 (1989) L2112, https://doi.org/10.1143/JJAP.28.L2112.
[19] S. Nakamura, N. Iwasa, M. Senoh, T. Mukai, Hole compensation mechanism of P-type GaN films, Jpn. J. Appl. Phys. 31 (1992) 1258, https://doi.org/10.1143/JJAP.31.1258.
[20] J. Neugebauer, C.G. Van de Walle, Hydrogen in GaN: novel aspects of a common impurity, Phys. Rev. Lett. 75 (1995) 4452–4455, https://doi.org/10.1103/PhysRevLett.75.4452.
[21] J. Neugebauer, C.G. Van de Walle, Role of hydrogen in doping of GaN, Appl. Phys. Lett. 68 (1996) 1829–1831, https://doi.org/10.1063/1.116027.
[22] S. Nakamura, T. Mukai, M. Senoh, N. Iwasa, Thermal annealing effects on P-type Mg-doped GaN films, Jpn. J. Appl. Phys. 31 (1992) L139, https://doi.org/10.1143/JJAP.31.L139.
[23] H.P. Maruska, D.A. Stevenson, J.J. Pankove, Violet luminescence of Mg-doped GaN, Appl. Phys. Lett. 22 (1973) 303–305, https://doi.org/10.1063/1.1654648.
[24] M. Ilegems, R. Dingle, Luminescence of Be- and Mg-doped GaN, J. Appl. Phys. 44 (1973) 4234–4235, https://doi.org/10.1063/1.1662930.
[25] MIS Type Blue LEDs with a Brightness of 200 mcd Were Developed by Toyoda Gosei, Nikkan Kogyo Shinbun Jpn. Newsp. Press Release, 1993.
[26] S. Nakamura, T. Mukai, M. Senoh, High-power GaN P–N junction blue-light-emitting diodes, Jpn. J. Appl. Phys. 30 (1991) L1998, https://doi.org/10.1143/JJAP.30.L1998.
[27] The Nobel prize in physics 2000, https://www.nobelprize.org/nobel_prizes/physics/laureates/2000/, 2000. (Accessed 14 November 2017).
[28] L.A. Coldren, S.W. Corzine, M.L. Mashanovitch, Diode Lasers and Photonic Integrated Circuits, John Wiley & Sons, 2012.
[29] T. Matsuoka, H. Tanaka, T. Sasaki, A. Katsui, Wide-gap semiconductor (In, Ga)N, in: Proc. 16th Int. Symposium on GaAs and Related Compounds, Karuizawa, Japan, 1989, in: Institute of Physics Conference Series, vol. 106, Institute of Physics, Bristol, UK, 1990, p. 141.
[30] M. Auf der Maur, A. Pecchia, G. Penazzi, W. Rodrigues, A. Di Carlo, Efficiency drop in green InGaN/GaN light emitting diodes: the role of random alloy fluctuations, Phys. Rev. Lett. 116 (2016) 027401, https://doi.org/10.1103/PhysRevLett.116.027401.
[31] M.R. Krames, O.B. Shchekin, R. Mueller-Mach, G.O. Mueller, L. Zhou, G. Harbers, M.G. Craford, Status and future of high-power light-emitting diodes for solid-state lighting, J. Disp. Technol. 3 (2007) 160–175, https://doi.org/10.1109/JDT.2007.895339.
[32] K. Osamura, K. Nakajima, Y. Murakami, P.H. Shingu, A. Ohtsuki, Fundamental absorption edge in GaN, InN and their alloys, Solid State Commun. 11 (1972) 617–621, https://doi.org/10.1016/0038-1098(72)90474-7.
[33] K. Osamura, S. Naka, Y. Murakami, Preparation and optical properties of $Ga_{1-x}In_xN$ thin films, J. Appl. Phys. 46 (1975) 3432–3437, https://doi.org/10.1063/1.322064.
[34] T. Nagatomo, T. Kuboyama, H. Minamino, O. Omoto, Properties of $Ga_{1-x}In_xN$ films prepared by MOVPE, Jpn. J. Appl. Phys. 28 (1989) L1334, https://doi.org/10.1143/JJAP.28.L1334.
[35] N. Yoshimoto, T. Matsuoka, T. Sasaki, A. Katsui, Photoluminescence of InGaN films grown at high temperature by metalorganic vapor phase epitaxy, Appl. Phys. Lett. 59 (1991) 2251–2253, https://doi.org/10.1063/1.106086.
[36] S. Nakamura, T. Mukai, High-quality InGaN films grown on GaN films, Jpn. J. Appl. Phys. 31 (1992) L1457, https://doi.org/10.1143/JJAP.31.L1457.
[37] S. Nakamura, M. Senoh, T. Mukai, P-GaN/N-InGaN/N-GaN double-heterostructure blue-light-emitting diodes, Jpn. J. Appl. Phys. 32 (1993) L8, https://doi.org/10.1143/JJAP.32.L8.
[38] S. Nakamura, M. Senoh, N. Iwasa, S. Nagahama, High-brightness InGaN blue, green and yellow light-emitting diodes with quantum well structures, Jpn. J. Appl. Phys. 34 (1995) L797, https://doi.org/10.1143/JJAP.34.L797.
[39] S. Nakamura, M. Senoh, N. Iwasa, S. Nagahama, T. Yamada, T. Mukai, Superbright green InGaN single-quantum-well-structure light-emitting diodes, Jpn. J. Appl. Phys. 34 (1995) L1332, https://doi.org/10.1143/JJAP.34.L1332.
[40] K. Bando, Y. Noguchi, K. Sakamoto, Y. Shimizu, in: Development and Application of High-Brightness White LEDs, 1996.
[41] K. Bando, K. Sakano, Y. Noguchi, Y. Shimizu, Development of high-bright and pure-white LED lamps, J. Light Vis. Environ. 22 (1998), https://doi.org/10.2150/jlve.22.1_2, 5pp.
[42] A. David, Surface-roughened light-emitting diodes: an accurate model, J. Disp. Technol. 9 (2013) 301–316, https://doi.org/10.1109/JDT.2013.2240373.
[43] T. Fujii, Y. Gao, R. Sharma, E.L. Hu, S.P. DenBaars, S. Nakamura, Increase in the extraction efficiency of GaN-based light-emitting diodes via surface roughening, Appl. Phys. Lett. 84 (2004) 855–857, https://doi.org/10.1063/1.1645992.
[44] M. Yamada, T. Mitani, Y. Narukawa, S. Shioji, I. Niki, S. Sonobe, K. Deguchi, M. Sano, T. Mukai, InGaN-based near-ultraviolet and blue-light-emitting diodes with high external quantum efficiency using a patterned sapphire substrate and a mesh electrode, Jpn. J. Appl. Phys. 41 (2002) L1431, https://doi.org/10.1143/JJAP.41.L1431.

[45] M.R. Krames, M. Ochiai-Holcomb, G.E. Höfler, C. Carter-Coman, E.I. Chen, I.-H. Tan, P. Grillot, N.F. Gardner, H.C. Chui, J.-W. Huang, S.A. Stockman, F.A. Kish, M.G. Craford, T.S. Tan, C.P. Kocot, M. Hueschen, J. Posselt, B. Loh, G. Sasser, D. Collins, High-power truncated-inverted-pyramid (AlxGa1−x)0.5In0.5P/GaP light-emitting diodes exhibiting >50% external quantum efficiency, Appl. Phys. Lett. 75 (1999) 2365–2367, https://doi.org/10.1063/1.125016.
[46] M. Ma, F.W. Mont, X. Yan, J. Cho, E.F. Schubert, G.B. Kim, C. Sone, Effects of the refractive index of the encapsulant on the light-extraction efficiency of light-emitting diodes, Opt. Express 19 (2011) A1135–A1140, https://doi.org/10.1364/OE.19.0A1135.
[47] C.L. Keraly, L. Kuritzky, M. Cochet, C. Weisbuch, Ray tracing for light extraction efficiency (LEE) modeling in nitride LEDs, in: III-Nitride Based Light Emit. Diodes Appl., Springer, Singapore, 2017, pp. 301–340.
[48] J.-Y. Kim, T. Jeong, S.H. Lee, H.S. Oh, H.J. Park, S.-M. Kim, J.H. Baek, Light extraction of high-efficient light-emitting diodes, in: III-Nitride Based Light Emit. Diodes Appl., Springer, Singapore, 2017, pp. 341–361.
[49] S.J. Chang, C.F. Shen, W.S. Chen, T.K. Ko, C.T. Kuo, K.H. Yu, S.C. Shei, Y.Z. Chiou, Nitride-based LEDs with an insulating SiO_2 layer underneath p-pad electrodes, Electrochem. Solid-State Lett. 10 (2007) H175–H177, https://doi.org/10.1149/1.2718392.
[50] D.A. Steigerwald, J.C. Bhat, D. Collins, R.M. Fletcher, M.O. Holcomb, M.J. Ludowise, P.S. Martin, S.L. Rudaz, Illumination with solid state lighting technology, IEEE J. Sel. Top. Quantum Electron. 8 (2002) 310–320, https://doi.org/10.1109/2944.999186.
[51] J.J. Wierer, D.A. Steigerwald, M.R. Krames, J.J. O'Shea, M.J. Ludowise, G. Christenson, Y.-C. Shen, C. Lowery, P.S. Martin, S. Subramanya, W. Götz, N.F. Gardner, R.S. Kern, S.A. Stockman, High-power AlGaInN flip-chip light-emitting diodes, Appl. Phys. Lett. 78 (2001) 3379–3381, https://doi.org/10.1063/1.1374499.
[52] W.S. Wong, T. Sands, N.W. Cheung, M. Kneissl, D.P. Bour, P. Mei, L.T. Romano, N.M. Johnson, Fabrication of thin-film InGaN light-emitting diode membranes by laser lift-off, Appl. Phys. Lett. 75 (1999) 1360–1362, https://doi.org/10.1063/1.124693.
[53] V. Haerle, B. Hahn, S. Kaiser, A. Weimar, S. Bader, F. Eberhard, A. Plössl, D. Eisert, High brightness LEDs for general lighting applications using the new ThinGaN™-technology, Phys. Status Solidi A 201 (2004) 2736–2739, https://doi.org/10.1002/pssa.200405119.
[54] P. Kumar, S.Y. Son, R. Singh, K. Balasundaram, J. Lee, R. Singh, Analytical treatment of light extraction from textured surfaces using classical ray optics, Opt. Commun. 284 (2011) 4874–4878, https://doi.org/10.1016/j.optcom.2011.06.062.
[55] O.B. Shchekin, J.E. Epler, T.A. Trottier, T. Margalith, D.A. Steigerwald, M.O. Holcomb, P.S. Martin, M.R. Krames, High performance thin-film flip-chip InGaN–GaN light-emitting diodes, Appl. Phys. Lett. 89 (2006) 071109, https://doi.org/10.1063/1.2337007.
[56] K. Tadatomo, H. Okagawa, Y. Ohuchi, T. Tsunekawa, Y. Imada, M. Kato, T. Taguchi, High output power InGaN ultraviolet light-emitting diodes fabricated on patterned substrates using metalorganic vapor phase epitaxy, Jpn. J. Appl. Phys. 40 (2001) L583, https://doi.org/10.1143/JJAP.40.L583.
[57] K. Tadatomo, Epitaxial growth of GaN on patterned sapphire substrates, in: III-Nitride Based Light Emit. Diodes Appl., Springer, Singapore, 2017, pp. 69–92.
[58] Y. Narukawa, M. Ichikawa, D. Sanga, M. Sano, T. Mukai, White light emitting diodes with super-high luminous efficacy, J. Phys. Appl. Phys. 43 (2010) 354002, https://doi.org/10.1088/0022-3727/43/35/354002.
[59] Kensaku MOTOK, Development of gallium nitride substrates, SEI Tech. Rev. 70 (2010) 28–35.
[60] H. Geng, H. Sunakawa, N. Sumi, K. Yamamoto, A. Atsushi Yamaguchi, A. Usui, Growth and strain characterization of high quality GaN crystal by HVPE, J. Cryst. Growth 350 (2012) 44–49, https://doi.org/10.1016/j.jcrysgro.2011.12.020.
[61] K. Fujito, S. Kubo, I. Fujimura, Development of bulk GaN crystals and nonpolar/semipolar substrates by HVPE, Mater. Res. Soc. Bull. 34 (2009) 313–317, https://doi.org/10.1557/mrs2009.92.
[62] D. Ehrentraut, R.T. Pakalapati, D.S. Kamber, W. Jiang, D.W. Pocius, B.C. Downey, M. McLaurin, M.P. D'Evelyn High, Quality, low cost ammonothermal bulk GaN substrates, Jpn. J. Appl. Phys. 52 (2013) 08JA01, https://doi.org/10.7567/JJAP.52.08JA01.
[63] C.A. Hurni, A. David, M.J. Cich, R.I. Aldaz, B. Ellis, K. Huang, A. Tyagi, R.A. DeLille, M.D. Craven, F.M. Steranka, M.R. Krames, Bulk GaN flip-chip violet light-emitting diodes with optimized efficiency for high-power operation, Appl. Phys. Lett. 106 (2015) 031101, https://doi.org/10.1063/1.4905873.
[64] M.J. Cich, R.I. Aldaz, A. Chakraborty, A. David, M.J. Grundmann, A. Tyagi, M. Zhang, F.M. Steranka, M.R. Krames, Bulk GaN based violet light-emitting diodes with high efficiency at very high current density, Appl. Phys. Lett. 101 (2012) 223509, https://doi.org/10.1063/1.4769228.
[65] J.Y. Kim, M.K. Kwon, J.P. Kim, S.J. Park, Enhanced light extraction from triangular GaN-based light-emitting diodes, IEEE Photonics Technol. Lett. 19 (2007) 1865–1867, https://doi.org/10.1109/LPT.2007.907644.
[66] A. David, C.A. Hurni, R.I. Aldaz, M.J. Cich, B. Ellis, K. Huang, F.M. Steranka, M.R. Krames, High light extraction efficiency in bulk-GaN based volumetric violet light-emitting diodes, Appl. Phys. Lett. 105 (2014) 231111, https://doi.org/10.1063/1.4903297.
[67] S.D. Lester, F.A. Ponce, M.G. Craford, D.A. Steigerwald, High dislocation densities in high efficiency GaN-based light-emitting diodes, Appl. Phys. Lett. 66 (1995) 1249–1251, https://doi.org/10.1063/1.113252.
[68] S. Nakamura, M. Senoh, N. Iwasa, S. Nagahama, High-power InGaN single-quantum-well-structure blue and violet light-emitting diodes, Appl. Phys. Lett. 67 (1995) 1868–1870, https://doi.org/10.1063/1.114359.
[69] S.F. Chichibu, A. Uedono, T. Onuma, B.A. Haskell, A. Chakraborty, T. Koyama, P.T. Fini, S. Keller, S.P. DenBaars, J.S. Speck, U.K. Mishra, S. Nakamura, S. Yamaguchi, S. Kamiyama, H. Amano, I. Akasaki, J. Han, T. Sota, Origin of defect-insensitive emission probability in In-containing (Al, In, Ga)N alloy semiconductors, Nat. Mater. 5 (2006) nmat1726, https://doi.org/10.1038/nmat1726.
[70] T.-J. Yang, R. Shivaraman, J.S. Speck, Y.-R. Wu, The influence of random indium alloy fluctuations in indium gallium nitride quantum wells on the device behavior, J. Appl. Phys. 116 (2014) 113104, https://doi.org/10.1063/1.4896103.
[71] S. Itoh, K. Nakano, A. Ishibashi, Current status and future prospects of ZnSe-based light-emitting devices, J. Cryst. Growth 214–215 (2000) 1029–1034, https://doi.org/10.1016/S0022-0248(00)00264-5.
[72] F. Bernardini, V. Fiorentini, D. Vanderbilt, Spontaneous polarization and piezoelectric constants of III–V nitrides, Phys. Rev. B 56 (1997) R10024–R10027, https://doi.org/10.1103/PhysRevB.56.R10024.
[73] V. Fiorentini, F. Bernardini, F. Della Sala, A. Di Carlo, P. Lugli, Effects of macroscopic polarization in III–V nitride multiple quantum wells, Phys. Rev. B 60 (1999) 8849–8858, https://doi.org/10.1103/PhysRevB.60.8849.
[74] A.E. Romanov, T.J. Baker, S. Nakamura, J.S. Speck, Strain-induced polarization in wurtzite III-nitride semipolar layers, J. Appl. Phys. 100 (2006) 023522, https://doi.org/10.1063/1.2218385.
[75] E. Kioupakis, Q. Yan, C.G.V. de Walle, Interplay of polarization fields and Auger recombination in the efficiency droop of nitride light-emitting diodes, Appl. Phys. Lett. 101 (2012) 231107, https://doi.org/10.1063/1.4769374.
[76] D.F. Feezell, J.S. Speck, S.P. DenBaars, S. Nakamura, Semipolar (20-2-1) InGaN/GaN light-emitting diodes for high-efficiency solid-state lighting, J. Disp. Technol. 9 (2013) 190–198, https://doi.org/10.1109/JDT.2012.2227682.
[77] Y.-R. Wu, R. Shivaraman, K.-C. Wang, J.S. Speck, Analyzing the physical properties of InGaN multiple quantum well light emitting diodes from nano scale structure, Appl. Phys. Lett. 101 (2012) 083505, https://doi.org/10.1063/1.4747532.
[78] C.K. Li, Y.R. Wu, Study on the current spreading effect and light extraction enhancement of vertical GaN/InGaN LEDs, IEEE Trans. Electron Devices 59 (2012) 400–407, https://doi.org/10.1109/TED.2011.2176132.
[79] P.G. Eliseev, M. Osin'ski, H. Li, I.V. Akimova, Recombination balance in green-light-emitting GaN/InGaN/AlGaN quantum wells, Appl. Phys. Lett. 75 (1999) 3838–3840, https://doi.org/10.1063/1.125473.
[80] A. David, M.J. Grundmann, Droop in InGaN light-emitting diodes: a differential carrier lifetime analysis, Appl. Phys. Lett. 96 (2010) 103504, https://doi.org/10.1063/1.3330870.

[81] Q. Dai, Q. Shan, J. Wang, S. Chhajed, J. Cho, E.F. Schubert, M.H. Crawford, D.D. Koleske, M.-H. Kim, Y. Park, Carrier recombination mechanisms and efficiency droop in GaInN/GaN light-emitting diodes, Appl. Phys. Lett. 97 (2010) 133507, https://doi.org/10.1063/1.3493654.
[82] C. Weisbuch, M. Piccardo, L. Martinelli, J. Iveland, J. Peretti, J.S. Speck, The efficiency challenge of nitride light-emitting diodes for lighting, Phys. Status Solidi A 212 (2015) 899–913, https://doi.org/10.1002/pssa.201431868.
[83] Y.C. Shen, G.O. Mueller, S. Watanabe, N.F. Gardner, A. Munkholm, M.R. Krames, Auger recombination in InGaN measured by photoluminescence, Appl. Phys. Lett. 91 (2007) 141101, https://doi.org/10.1063/1.2785135.
[84] J. Iveland, L. Martinelli, J. Peretti, J.S. Speck, C. Weisbuch, Direct measurement of Auger electrons emitted from a semiconductor light-emitting diode under electrical injection: identification of the dominant mechanism for efficiency droop, Phys. Rev. Lett. 110 (2013) 177406, https://doi.org/10.1103/PhysRevLett.110.177406.
[85] K.-S. Kim, D.-P. Han, H.-S. Kim, J.-I. Shim, Analysis of dominant carrier recombination mechanisms depending on injection current in InGaN green light emitting diodes, Appl. Phys. Lett. 104 (2014) 091110, https://doi.org/10.1063/1.4867647.
[86] M.-H. Kim, M.F. Schubert, Q. Dai, J.K. Kim, E.F. Schubert, J. Piprek, Y. Park, Origin of efficiency droop in GaN-based light-emitting diodes, Appl. Phys. Lett. 91 (2007) 183507, https://doi.org/10.1063/1.2800290.
[87] J. Hader, J.V. Moloney, S.W. Koch, Temperature-dependence of the internal efficiency droop in GaN-based diodes, Appl. Phys. Lett. 99 (2011) 181127, https://doi.org/10.1063/1.3658031.
[88] D.-S. Shin, D.-P. Han, J.-Y. Oh, J.-I. Shim, Study of droop phenomena in InGaN-based blue and green light-emitting diodes by temperature-dependent electroluminescence, Appl. Phys. Lett. 100 (2012) 153506, https://doi.org/10.1063/1.3703313.
[89] N.F. Gardner, G.O. Müller, Y.C. Shen, G. Chen, S. Watanabe, W. Götz, M.R. Krames, Blue-emitting InGaN–GaN double-heterostructure light-emitting diodes reaching maximum quantum efficiency above 200 A/cm^2, Appl. Phys. Lett. 91 (2007) 243506, https://doi.org/10.1063/1.2807272.
[90] A. Laubsch, M. Sabathil, W. Bergbauer, M. Strassburg, H. Lugauer, M. Peter, S. Lutgen, N. Linder, K. Streubel, J. Hader, J.V. Moloney, B. Pasenow, S.W. Koch, On the origin of IQE-'droop' in InGaN LEDs, Phys. Status Solidi C 6 (2009) S913–S916, https://doi.org/10.1002/pssc.200880950.
[91] A. David, M.J. Grundmann, Influence of polarization fields on carrier lifetime and recombination rates in InGaN-based light-emitting diodes, Appl. Phys. Lett. 97 (2010) 033501, https://doi.org/10.1063/1.3462916.
[92] M. Binder, A. Nirschl, R. Zeisel, T. Hager, H.-J. Lugauer, M. Sabathil, D. Bougeard, J. Wagner, B. Galler, Identification of nnp and npp Auger recombination as significant contributor to the efficiency droop in (GaIn)N quantum wells by visualization of hot carriers in photoluminescence, Appl. Phys. Lett. 103 (2013) 071108, https://doi.org/10.1063/1.4818761.
[93] E. Kioupakis, P. Rinke, K.T. Delaney, C.G. Van de Walle, Indirect Auger recombination as a cause of efficiency droop in nitride light-emitting diodes, Appl. Phys. Lett. 98 (2011) 161107, https://doi.org/10.1063/1.3570656.
[94] E. Kioupakis, D. Steiauf, P. Rinke, K.T. Delaney, C.G. Van de Walle, First-principles calculations of indirect Auger recombination in nitride semiconductors, Phys. Rev. B 92 (2015) 035207, https://doi.org/10.1103/PhysRevB.92.035207.
[95] E. Kioupakis, Q. Yan, D. Steiauf, C.G.V. de Walle, Temperature and carrier-density dependence of Auger and radiative recombination in nitride optoelectronic devices, New J. Phys. 15 (2013) 125006, https://doi.org/10.1088/1367-2630/15/12/125006.
[96] M. Deppner, F. Römer, B. Witzigmann, Auger carrier leakage in III-nitride quantum-well light emitting diodes, Phys. Status Solidi RRL 6 (2012) 418–420, https://doi.org/10.1002/pssr.201206367.
[97] J. Iveland, M. Piccardo, L. Martinelli, J. Peretti, J.W. Choi, N. Young, S. Nakamura, J.S. Speck, C. Weisbuch, Origin of electrons emitted into vacuum from InGaN light emitting diodes, Appl. Phys. Lett. 105 (2014) 052103, https://doi.org/10.1063/1.4892473.
[98] J. Peretti, C. Weisbuch, J. Iveland, M. Piccardo, L. Martinelli, J.S. Speck, Identification of Auger effect as the dominant mechanism for efficiency droop of LEDs, in: Proc. SPIE, 9003, International Society for Optics and Photonics, 2014, p. 90030Z.
[99] J. Piprek, Efficiency droop in nitride-based light-emitting diodes, Phys. Status Solidi A 207 (2010) 2217–2225, https://doi.org/10.1002/pssa.201026149.
[100] J.-I. Shim, Internal quantum efficiency, in: III-Nitride Based Light Emit. Diodes Appl, Springer, Singapore, 2017, pp. 163–207.
[101] J. Cho, E.F. Schubert, J.K. Kim, Efficiency droop in light-emitting diodes: challenges and countermeasures, Laser Photonics Rev. 7 (2013) 408–421, https://doi.org/10.1002/lpor.201200025.
[102] A. David, M.J. Grundmann, J.F. Kaeding, N.F. Gardner, T.G. Mihopoulos, M.R. Krames, Carrier distribution in (0001)InGaN/GaN multiple quantum well light-emitting diodes, Appl. Phys. Lett. 92 (2008) 053502, https://doi.org/10.1063/1.2839305.
[103] C.-K. Li, M. Piccardo, L.-S. Lu, S. Mayboroda, L. Martinelli, J. Peretti, J.S. Speck, C. Weisbuch, M. Filoche, Y.-R. Wu, Localization landscape theory of disorder in semiconductors. III. Application to carrier transport and recombination in light emitting diodes, Phys. Rev. B 95 (2017) 144206, https://doi.org/10.1103/PhysRevB.95.144206.
[104] F. Akyol, S. Krishnamoorthy, S. Rajan, Tunneling-based carrier regeneration in cascaded GaN light emitting diodes to overcome efficiency droop, Appl. Phys. Lett. 103 (2013) 081107, https://doi.org/10.1063/1.4819737.
[105] S. Rajan, T. Takeuchi, III-Nitride tunnel junctions and their applications, in: III-Nitride Based Light Emit. Diodes Appl., Springer, Singapore, 2017, pp. 209–238.
[106] M. Malinverni, D. Martin, N. Grandjean, InGaN based micro light emitting diodes featuring a buried GaN tunnel junction, Appl. Phys. Lett. 107 (2015) 051107, https://doi.org/10.1063/1.4928037.
[107] D. Takasuka, Y. Akatsuka, M. Ino, N. Koide, T. Takeuchi, M. Iwaya, S. Kamiyama, I. Akasaki, GaInN-based tunnel junctions with graded layers, Appl. Phys. Express 9 (2016) 081005, https://doi.org/10.7567/APEX.9.081005.
[108] E.C. Young, B.P. Yonkee, F. Wu, S.H. Oh, S.P. DenBaars, S. Nakamura, J.S. Speck, Hybrid tunnel junction contacts to III-nitride light-emitting diodes, Appl. Phys. Express 9 (2016) 022102, https://doi.org/10.7567/APEX.9.022102.
[109] B.P. Yonkee, E.C. Young, S.P. DenBaars, S. Nakamura, J.S. Speck, Silver free III-nitride flip chip light-emitting-diode with wall plug efficiency over 70% utilizing a GaN tunnel junction, Appl. Phys. Lett. 109 (2016) 191104, https://doi.org/10.1063/1.4967501.
[110] J.T. Leonard, E.C. Young, B.P. Yonkee, D.A. Cohen, T. Margalith, S.P. DenBaars, J.S. Speck, S. Nakamaura, Demonstration of a III-nitride vertical-cavity surface-emitting laser with a III-nitride tunnel junction intracavity contact, Appl. Phys. Lett. 107 (2015) 091105, https://doi.org/10.1063/1.4929944.
[111] B.P. Yonkee, E.C. Young, C. Lee, J.T. Leonard, S.P. DenBaars, J.S. Speck, S. Nakamura, Demonstration of a III-nitride edge-emitting laser diode utilizing a GaN tunnel junction contact, Opt. Express 24 (2016) 7816–7822, https://doi.org/10.1364/OE.24.007816.
[112] M. Monavarian, A. Rashidi, A. Aragon, S.H. Oh, M. Nami, S.P. DenBaars, D. Feezell, Explanation of low efficiency droop in semipolar (20-2-1) InGaN/GaN LEDs through evaluation of carrier recombination coefficients, Opt. Express 25 (2017) 19343–19353, https://doi.org/10.1364/OE.25.019343.
[113] Y. Kawaguchi, C.-Y. Huang, Y.-R. Wu, Q. Yan, C.-C. Pan, Y. Zhao, S. Tanaka, K. Fujito, D. Feezell, C.G.V. de Walle, S.P. DenBaars, S. Nakamaura, Influence of polarity on carrier transport in semipolar (202-1) and (20-2-1) multiple-quantum-well light-emitting diodes, Appl. Phys. Lett. 100 (2012) 231110, https://doi.org/10.1063/1.4726106.
[114] A. David, N.F. Gardner, Droop in III-nitrides: comparison of bulk and injection contributions, Appl. Phys. Lett. 97 (2010) 193508, https://doi.org/10.1063/1.3515851.
[115] A.M. Armstrong, B.N. Bryant, M.H. Crawford, D.D. Koleske, S.R. Lee, J.J. Wierer, Defect-reduction mechanism for improving radiative efficiency in InGaN/GaN light-emitting diodes using InGaN underlayers, J. Appl. Phys. 117 (2015) 134501, https://doi.org/10.1063/1.4916727.
[116] J.Y. Tsao, H.D. Saunders, J.R. Creighton, M.E. Coltrin, J.A. Simmons, Solid-state lighting: an energy-economics perspective, J. Phys. Appl. Phys. 43 (2010) 354001, https://doi.org/10.1088/0022-3727/43/35/354001.

[117] R. Haitz, J.Y. Tsao, Solid-state lighting: 'the case' 10 years after and future prospects, Phys. Status Solidi A 208 (2011) 17–29, https://doi.org/10.1002/pssa.201026349.
[118] J. Cho, J.H. Park, J.K. Kim, E.F. Schubert, White light-emitting diodes: history, progress, and future, Laser Photonics Rev. 11 (2017), https://doi.org/10.1002/lpor.201600147.
[119] Y. Shimizu, Japanese patent application publication H08-7614, 1996.
[120] Y. Shimizu, K. Sakano, Y. Noguchi, T. Moriguchi, Japanese priority patent applications to U.S, 1999, patent 5,998,925.
[121] High Color-Rendering, Full-visible-spectrum LEDs by Soraa — LED professional - LED lighting technology, application magazine, https://www.led-professional.com/resources-1/articles/high-color-rendering-full-visible-spectrum-leds-the-first-wave-of-conventional-white-leds-primarily-focused-on-lumens-per-watt-these-leds-were-by-soraa, 2016. (Accessed 15 November 2017).
[122] SORAA, https://www.soraa.com/news_releases/31, 2015. (Accessed 15 November 2017).
[123] DOE Solid-State Lighting R&D Plan, https://energy.gov/sites/prod/files/2016/06/f32/ssl_rd-plan_%20jun2016_2.pdf, 2016. (Accessed 14 November 2017).
[124] G. Craford, Innovations in LEDs, https://www.energy.gov/sites/prod/files/2015/02/f19/craford_innovation_sanfrancisco2015.pdf, 2015.
[125] J.M. Phillips, M.E. Coltrin, M.H. Crawford, A.J. Fischer, M.R. Krames, R. Mueller-Mach, G.O. Mueller, Y. Ohno, L.E.S. Rohwer, J.A. Simmons, J.Y. Tsao, Research challenges to ultra-efficient inorganic solid-state lighting, Laser Photonics Rev. 1 (2007) 307–333, https://doi.org/10.1002/lpor.200710019.
[126] A.I. Alhassan, R.M. Farrell, B. Saifaddin, A. Mughal, F. Wu, S.P. DenBaars, S. Nakamura, J.S. Speck, High luminous efficacy green light-emitting diodes with AlGaN cap layer, Opt. Express 24 (2016) 17868–17873, https://doi.org/10.1364/OE.24.017868.
[127] Osram achieves record figures with green LEDs | OSRAM opto semiconductors, http://www.osram-os.com/osram_os/en/press/press-releases/led-for-automotive,-consumer,-industry/2014/osram-achieves-record-figures-with-green-leds/index.jsp, 2014. (Accessed 15 November 2017).
[128] Y. Narukawa, White-light LEDS, Opt. Photonics News 15 (2004) 24–29, https://doi.org/10.1364/OPN.15.4.000024.
[129] Y. Narukawa, J. Narita, T. Sakamoto, K. Deguchi, T. Yamada, T. Mukai, Ultra-high efficiency white light emitting diodes, Jpn. J. Appl. Phys. 45 (2006) L1084, https://doi.org/10.1143/JJAP.45.L1084.
[130] Cree Breaks 200 Lumen Per Watt Efficacy Barrier, http://www.cree.com/news-media/news/article/cree-breaks-200-lumen-per-watt-efficacy-barrier, 2010. (Accessed 14 November 2017).
[131] A. Michiue, T. Miyoshi, T. Yanamoto, T. Kozaki, S. Nagahama, Y. Narukawa, M. Sano, T. Yamada, T. Mukai, Recent development of nitride LEDs and LDs, in: Proc. SPIE, 7216, International Society for Optics and Photonics, 2009, p. 72161Z.
[132] Osram constructs the world's most efficient LED lamp | OSRAM, http://www.osram.com.au/osram_au/press/press-releases/_trade_press/2014/osram-constructs-the-worlds-most-efficient-led-lamp/index.jsp, 2014. (Accessed 15 November 2017).
[133] Cree First to Break 300 Lumens-Per-Watt Barrier, http://www.cree.com/news-events/news/article/cree-first-to-break-300-lumens-per-watt-barrier, 2014. (Accessed 14 November 2017).
[134] R.F. Karlicek, Emerging system level applications for LED technology, in: III-Nitride Based Light Emit. Diodes Appl., Springer, Singapore, 2017, pp. 481–492.
[135] C.X. Wang, F. Haider, X. Gao, X.H. You, Y. Yang, D. Yuan, H.M. Aggoune, H. Haas, S. Fletcher, E. Hepsaydir, Cellular architecture and key technologies for 5G wireless communication networks, IEEE Commun. Mag. 52 (2014) 122–130, https://doi.org/10.1109/MCOM.2014.6736752.
[136] S. Rajbhandari, J.J.D. McKendry, J. Herrnsdorf, H. Chun, G. Faulkner, H. Haas, I.M. Watson, D. O'Brien, M.D. Dawson, A review of gallium nitride LEDs for multi-gigabit-per-second visible light data communications, Semicond. Sci. Technol. 32 (2017) 023001, https://doi.org/10.1088/1361-6641/32/2/023001.
[137] M. Ayyash, H. Elgala, A. Khreishah, V. Jungnickel, T. Little, S. Shao, M. Rahaim, D. Schulz, J. Hilt, R. Freund, Coexistence of WiFi and LiFi toward 5G: concepts, opportunities, and challenges, IEEE Commun. Mag. 54 (2016) 64–71, https://doi.org/10.1109/MCOM.2016.7402263.
[138] H. Haas, L. Yin, Y. Wang, C. Chen, What is LiFi?, J. Lightwave Technol. 34 (2016) 1533–1544, https://doi.org/10.1109/JLT.2015.2510021.
[139] S. Wu, H. Wang, C.H. Youn, Visible light communications for 5G wireless networking systems: from fixed to mobile communications, IEEE Netw. 28 (2014) 41–45, https://doi.org/10.1109/MNET.2014.6963803.
[140] D. O'Brien, G. Parry, P. Stavrinou, Optical hotspots speed up wireless communication, Nat. Photonics 1 (2007) 245–247, https://doi.org/10.1038/nphoton.2007.52.
[141] A. Rashidi, M. Monavarian, A. Aragon, S. Okur, M. Nami, A. Rishinaramangalam, S. Mishkat-Ul-Masabih, D. Feezell, High-speed nonpolar InGaN/GaN LEDs for visible-light communication, IEEE Photonics Technol. Lett. 29 (2017) 381–384, https://doi.org/10.1109/LPT.2017.2650681.
[142] R.X.G. Ferreira, E. Xie, J.J.D. McKendry, S. Rajbhandari, H. Chun, G. Faulkner, S. Watson, A.E. Kelly, E. Gu, R.V. Penty, I.H. White, D.C. O'Brien, M.D. Dawson, High bandwidth GaN-based micro-LEDs for multi-gb/s visible light communications, IEEE Photonics Technol. Lett. 28 (2016) 2023–2026, https://doi.org/10.1109/LPT.2016.2581318.
[143] J.W. Shi, K.L. Chi, J.M. Wun, J.E. Bowers, Y.H. Shih, J.K. Sheu, III-Nitride-based cyan light-emitting diodes with GHz bandwidth for high-speed visible light communication, IEEE Electron Device Lett. 37 (2016) 894–897, https://doi.org/10.1109/LED.2016.2573265.
[144] J.J.D. McKendry, R.P. Green, A.E. Kelly, Z. Gong, B. Guilhabert, D. Massoubre, E. Gu, M.D. Dawson, High-speed visible light communications using individual pixels in a micro light-emitting diode array, IEEE Photonics Technol. Lett. 22 (2010) 1346–1348, https://doi.org/10.1109/LPT.2010.2056360.
[145] C.L. Liao, Y.F. Chang, C.L. Ho, M.C. Wu, High-speed GaN-based blue light-emitting diodes with gallium-doped ZnO current spreading layer, IEEE Electron Device Lett. 34 (2013) 611–613, https://doi.org/10.1109/LED.2013.2252457.
[146] Z. Quan, D.V. Dinh, S. Presa, B. Roycroft, A. Foley, M. Akhter, D. O'Mahony, P.P. Maaskant, M. Caliebe, F. Scholz, P.J. Parbrook, B. Corbett, High bandwidth freestanding semipolar (11-22) InGaN/GaN light-emitting diodes, IEEE Photonics J. 8 (2016) 1–8, https://doi.org/10.1109/JPHOT.2016.2596245.
[147] J.J.D. McKendry, D. Massoubre, S. Zhang, B.R. Rae, R.P. Green, E. Gu, R.K. Henderson, A.E. Kelly, M.D. Dawson, Visible-light communications using a CMOS-controlled micro-light- emitting-diode array, J. Lightwave Technol. 30 (2012) 61–67, https://doi.org/10.1109/JLT.2011.2175090.
[148] A. Rashidi, M. Nami, M. Monavarian, A. Aragon, K. DaVico, F. Ayoub, S. Mishkat-Ul-Masabih, A. Rishinaramangalam, D. Feezell, Differential carrier lifetime and transport effects in electrically injected III-nitride light-emitting diodes, J. Appl. Phys. 122 (2017) 035706, https://doi.org/10.1063/1.4994648.
[149] A. David, C.A. Hurni, N.G. Young, M.D. Craven, Carrier dynamics and Coulomb-enhanced capture in III-nitride quantum heterostructures, Appl. Phys. Lett. 109 (2016) 033504, https://doi.org/10.1063/1.4959143.
[150] S. Nakamura, M. Senoh, S. Nagahama, N. Iwasa, T. Yamada, T. Matsushita, H. Kiyoku, Y. Sugimoto, InGaN-based multi-quantum-well-structure laser diodes, Jpn. J. Appl. Phys. 35 (1996) L74, https://doi.org/10.1143/JJAP.35.L74.
[151] S. Nakamura, M. Senoh, S. Nagahama, N. Iwasa, T. Yamada, T. Matsushita, Y. Sugimoto, H. Kiyoku, Room-temperature continuous-wave operation of InGaN multi-quantum-well structure laser diodes, Appl. Phys. Lett. 69 (1996) 4056–4058, https://doi.org/10.1063/1.117816.
[152] S. Nakamura, M. Senoh, S. Nagahama, N. Iwasa, T. Matsushita, T. Mukai, Blue InGaN-based laser diodes with an emission wavelength of 450 nm, Appl. Phys. Lett. 76 (1999) 22–24, https://doi.org/10.1063/1.125643.
[153] S. Nozaki, S. Yoshida, K. Yamanaka, O. Imafuji, S. Takigawa, T. Katayama, T. Tanaka, High-power and high-temperature operation of an InGaN laser over 3 W at 85 °C using a novel double-heat-flow packaging technology, Jpn. J. Appl. Phys. 55 (2016) 04EH05, https://doi.org/10.7567/JJAP.55.04EH05.
[154] M. Kawaguchi, O. Imafuji, S. Nozaki, H. Hagino, S. Takigawa, T. Katayama, T. Tanaka, Optical-loss suppressed InGaN laser diodes using undoped thick waveguide structure, in: Proc. SPIE, 9748, International Society for Optics and Photonics, 2016, p. 974818.
[155] U. Strauß, T. Hager, G. Brüderl, T. Wurm, A. Somers, C. Eichler, C. Vierheilig, A. Löffler, J. Ristic, A. Avramescu, Recent advances in c-plane GaN visible lasers, in: Proc. SPIE, 8986, International Society for Optics and Photonics, 2014, p. 89861L.

[156] S. Masui, Y. Nakatsu, D. Kasahara, S. Nagahama, Recent improvement in nitride lasers, in: Proc. SPIE, 1014, International Society for Optics and Photonics, 2017, p. 101041H.
[157] James Raring (Soraa Laser), Laser Diodes for Next Generation Light Sources, https://energy.gov/sites/prod/files/2016/02/f29/raring_leddroop_raleigh2016.pdf, 2016. (Accessed 15 November 2017).
[158] J.J. Wierer, J.Y. Tsao, D.S. Sizov, Comparison between blue lasers and light-emitting diodes for future solid-state lighting, Laser Photonics Rev. 7 (2013) 963–993, https://doi.org/10.1002/lpor.201300048.
[159] J.Y. Tsao, M.H. Crawford, M.E. Coltrin, A.J. Fischer, D.D. Koleske, G.S. Subramania, G.T. Wang, J.J. Wierer, R.F. Karlicek, Toward smart and ultra-efficient solid-state lighting, Adv. Opt. Mater. 2 (2014) 809–836, https://doi.org/10.1002/adom.201400131.
[160] J.J. Wierer, J.Y. Tsao, D.S. Sizov, The potential of III-nitride laser diodes for solid-state lighting, Phys. Status Solidi C 11 (2014) 674–677, https://doi.org/10.1002/pssc.201300422.
[161] W.W. Chow, M.H. Crawford, Analysis of lasers as a solution to efficiency droop in solid-state lighting, Appl. Phys. Lett. 107 (2015) 141107, https://doi.org/10.1063/1.4932582.
[162] C. Lee, C. Shen, H.M. Oubei, M. Cantore, B. Janjua, T.K. Ng, R.M. Farrell, M.M. El-Desouki, J.S. Speck, S. Nakamura, B.S. Ooi, S.P. DenBaars, 2 Gbit/s data transmission from an unfiltered laser-based phosphor-converted white lighting communication system, Opt. Express 23 (2015) 29779–29787, https://doi.org/10.1364/OE.23.029779.
[163] C. Lee, C. Zhang, M. Cantore, R.M. Farrell, S.H. Oh, T. Margalith, J.S. Speck, S. Nakamura, J.E. Bowers, S.P. DenBaars, 4 Gbps direct modulation of 450 nm GaN laser for high-speed visible light communication, Opt. Express 23 (2015) 16232–16237, https://doi.org/10.1364/OE.23.016232.
[164] Laser light for headlights: latest trend in car lighting | OSRAM Automotive, (n.d.). https://www.osram.com/am/specials/trends-in-automotive-lighting/laser-light-new-headlight-technology/index.jsp. (Accessed 16 November 2017).
[165] A. Neumann, J.J. Wierer, W. Davis, Y. Ohno, S.R.J. Brueck, J.Y. Tsao, Four-color laser white illuminant demonstrating high color-rendering quality, Opt. Express 19 (2011) A982–A990, https://doi.org/10.1364/OE.19.00A982.
[166] M. Peters, V. Rossin, B. Acklin, High-efficiency high-reliability laser diodes at JDS uniphase, in: Proc. SPIE, 5711, International Society for Optics and Photonics, 2005, pp. 142–152.
[167] P.A. Crump, M. Grimshaw, J. Wang, W. Dong, S. Zhang, S. Das, J. Farmer, M. DeVito, L.S. Meng, J.K. Brasseur, 85% power conversion efficiency 975-nm broad area diode lasers at −50 °C, 76% at 10 °C, in: Conf. Lasers Electro-Opt. Electron. Laser Sci. Conf. Photonic Appl. Syst. Technol. 2006 Pap. JWB24, Optical Society of America, 2006, p. JWB24, https://www.osapublishing.org/abstract.cfm?uri=QELS-2006-JWB24. (Accessed 15 November 2017).
[168] E.J. Radauscher, M. Meitl, C. Prevatte, S. Bonafede, R. Rotzoll, D. Gomez, T. Moore, B. Raymond, R. Cok, A. Fecioru, A.J. Trindade, B. Fisher, S. Goodwin, P. Hines, G. Melnik, S. Barnhill, C.A. Bower, Miniaturized LEDs for flat-panel displays, in: Proc. SPIE, 10124, International Society for Optics and Photonics, 2017, p. 1012418.
[169] C.-M. Kang, D.-J. Kong, J.-P. Shim, S. Kim, S.-B. Choi, J.-Y. Lee, J.-H. Min, D.-J. Seo, S.-Y. Choi, D.-S. Lee, Fabrication of a vertically-stacked passive-matrix micro-LED array structure for a dual color display, Opt. Express 25 (2017) 2489–2495, https://doi.org/10.1364/OE.25.002489.
[170] J. Day, J. Li, D.Y.C. Lie, C. Bradford, J.Y. Lin, H.X. Jiang, III-nitride full-scale high-resolution microdisplays, Appl. Phys. Lett. 99 (2011) 031116, https://doi.org/10.1063/1.3615679.
[171] K. Kishino, K. Nagashima, K. Yamano, Monolithic integration of InGaN-based nanocolumn light-emitting diodes with different emission colors, Appl. Phys. Express 6 (2012) 012101, https://doi.org/10.7567/APEX.6.012101.
[172] B. Monemar, B.J. Ohlsson, N.F. Gardner, L. Samuelson, Chapter seven – Nanowire-based visible light emitters, present status and outlook, in: S.A. Dayeh, A. Fontcuberta i Morral, C. Jagadish (Eds.), Semicond. Semimet., Elsevier, 2016, pp. 227–271.
[173] M. Nami, R.F. Eller, S. Okur, A.K. Rishinaramangalam, S. Liu, I. Brener, D.F. Feezell, Tailoring the morphology and luminescence of GaN/InGaN core–shell nanowires using bottom-up selective-area epitaxy, Nanotechnology 28 (2017) 025202, https://doi.org/10.1088/0957-4484/28/2/025202.
[174] Google Invests 15 Million USD in University Spin-out Focused on Micro LED Technology – LEDinside (2017). http://www.ledinside.com/news/2017/8/google_invests_15_million_usd_in_university_spin_out_focused_on_micro_led_technology. (Accessed 16 November 2017).
[175] Apple's Micro-LED Display Could Replace OLED Screens in Wearable Devices – LEDinside (2015). http://www.ledinside.com/news/2015/7/apples_micro_led_display_could_replace_oled_screens_in_wearable_devices. (Accessed 16 November 2017).